The effect of chemical composition and morphology on the properties of polyolefin films

Johannes Lodewiekus Barnard

Thesis presented in partial fulfilment of the requirements for the degree of Master of Science in the Faculty of Science at Stellenbosch University

Supervisor: Prof A.J. van Reenen

March 2018

Declaration

By submitting this thesis electronically, I declare that the entirety of the work contained therein is my own, original work, that I am the sole author thereof (save to the extent explicitly otherwise stated), that reproduction and publication thereof by Stellenbosch University will not infringe any third-party rights and that I have not previously in its entirety or in part submitted it for obtaining any qualification.

March 2018

Dedicated to my family Vic, Mandi and Yolandi

for all your love and support.

Summary

This thesis consists of three parts, in the first part a preliminary study was conducted pertaining to dunnage bags. Dunnage bags are large inflatable restraining devices used in containers to keep the cargo from toppling over when in transit. Dunnage bags currently in use consist of two materials; one of polyethylene (PE) for air permeability resistance and polypropylene (PP) for strength. In an attempt to create a single layer dunnage bag a material had to be selected having various properties such as high strength, puncture resistance and air permeability resistance. After preliminary testing it was found that high impact polypropylene (HIPP) or heterophasic ethylene-propylene copolymers (HEPCs) conformed to most of the required properties and were therefore selected as ideal candidate materials for further testing. HEPCs are readily available and widely used in various industries. The copolymer consists of an extremely complex composition consisting of PP and PE homopolymers as well as ethylene-propylene copolymers creating rubbery phases. Mechanical properties of this material are well known, but research into how polyethylene inclusion contribute to its permeability properties is still in its infancy. The concepts and problems introduced through answering this problem led to part two.

Part two served as the main part of the study and dealt with observation of the finer material properties on a molecular level which related to the macroscopic properties of the final product. The gas permeability of a series of HEPCs with varying ethylene content (sampled by online time-dependent extraction) were investigated and attempts were made to relate this macroscopic property to how ethylene inclusion affects the morphology. This was done by using various analytical techniques such as permeability testing, differential scanning calorimetry (DSC), positron annihilation lifetime spectroscopy (PALS), X-ray diffraction spectroscopy (XRD) and polarizing optical microscopy (POM). Crystal morphology and crystallization kinetics as well as polymer composition turned out to have a contribution towards the final permeability properties.

In part three these techniques were employed on a different sample set to substantiate the conclusions made in part two. A HDPE:LDPE blend with varying LDPE composition was studied. Interesting findings were made and substantiated by a PALS experiment. Part three agreed with the findings made in part two and a promising way of predicting the permeability of a polymeric film with varying chemical composition was achieved.

Opsomming

Hierdie tesis bestaan uit drie dele, in die eerste deel was ‘n voorlopige studie gedoen met betrekking tot dunnage sakke. Dunnage sakke is groot opblaasbare sakke wat vragte in houers keer om te tuimel gedurende die vervoer daarvan. Dunnage sakke bestaan huidiglik uit twee materiale; een van poliëtileen (PE) vir weerstand teen lugdeurlaatbaarheid en polipropileen (PP) vir sterkte. In 'n poging om 'n enkele laag dunnage sak te skep, moes 'n materiaal gekies word wat bestaan uit verskeie parameters soos hoë sterkte, punksieweerstand en lugdeurlaatbaarheid. Na voorlopige toetsing is bevind dat hoë impak polypropyleen (HIPP) of heterofasiese etileen-propileen kopolimere (HEPKs) uit die gunstigste eienskappe bevat, en daarom as ideale kandidaat-materiaal gekies is vir verdere toetsing. HEPK's is maklik bekombaar en word in verskeie nywerhede gebruik. Die kopolimeer bestaan uit 'n uiters komplekse samestelling, wat PP en PE homopolimeer en asook etileen-propileen kopolimere bevat wat rubberagtige fases skep. Meganiese eienskappe van hierdie materiaal is welbekend, maar navorsing oor hoe poliëtileen-insluitingby dra tot die deurlaatbaarheidseienskappe, is nog in sy kinderskoene. Die konsepte en probleme wat gestel is deur die probleem te beantwoord, het tot deel twee gelei.

Deel twee het gedien as die hoofdeel van die studie en het aandag gegee aan die waarneming van fyner materiaal eienskappe op molekulêre vlak wat verband hou met die makroskopiese eienskappe van die finale produk. Die gasdeurlaatbaarheid van 'n reeks HEPK's met wisselende etileeninhoud (ingesamel deur aanlyn tydafhanklike ekstraksie) is ondersoek. 'n Poging is aangewend om hierdie makroskopiese eienskap te vergelyk met hoe etileen-insluiting die morfologie beïnvloed. Dit is gedoen deur gebruik te maak van verskeie analitiese tegnieke soos deurlaatbaarheidstoetsing, differensiële skanderingskalorimetrie (DSK), positronvernietiging leeftyd spektroskopie (PVLS), X-straal diffraksie spektroskopie (XRD) sowel as gepolariserende optiese mikroskopie (POM). Kristal morfologie en kristallisasie kinetika sowel as polimeer samestelling blyk om 'n bydrae te lewer tot die finale deurlaatbaarheidseienskappe.

In deel drie is die tegnieke wat in deel 2 ontwikkel is toegepas op 'n nuwe stel polimere om die gevolgtrekkings in deel twee te staaf. 'n HDPE:LDPE mengsel met verskillende LDPE samestelling is bestudeer. Interessante bevindinge is gemaak en gestaaf deur 'n PVLS-eksperiment. Deel drie het ooreengekom met die bevindinge wat in deel twee gemaak is en 'n

belowende manier om die deurlaatbaarheid van 'n polimeerfilm met verskillende chemiese samestelling te voorspel, is behaal.

Acknowledgements

Prof. A.J. van Reenen (supervisor), for his guidance, patience, interest, enthusiasm, attention to detail and open door policy.

To Anderson Lid Company for the project and funding thereof.

Dr. D. Robertson for his continuous guidance, insets and mentorship.

Mr N. Basson for helping with PALS and XRD experimentation and data analysis.

To the rest of the polyolefin research group for their assistance and enthusiasm.

Also to family and friends for their moral support.

Table of Contents

List of tables:

List of figures:

List of equations:

List of abbreviations:

ABS	acrylonitrile butadiene styrene
DSC	differential scanning calorimetry
EVOH	ethylene-co-vinyl alcohol
HDPE	high density polyethylene
HEPC	heterophasic ethylene-propylene copolymers
iPP	isotactic polypropylene
LDPE	low density polyethylene
PA	polyamide
PALS	positron annihilation lifetime spectroscopy
PAN	polyacrylonitrile
PBT	polybutylene terephthalate
PC	polycarbonate
PEI	polyetherimide
PET	polyethylene terephthalate
PETG	polyethylene terephthalate glycol
POM	polarized-light optical microscopy
PP	polypropylene
PPE	polyphenylene ether
PPO	polyphenylene oxide
PVC	polyvinyl chloride

PVDC	polyvinylidene chloride
PBT	polybutylene terephthalate
XRD	x-ray diffraction

Part I: Preliminary study.

Chapter 1

1.1 Motivation of study

1.1.1 Aim and Objective: Dunnage bags

The aim of part one was to create a dunnage bag for industrial use. Dunnage bags are large inflatable restraining devices used to secure goods in multi-modal containers. These products consist of two major parts namely a thin, compliant, airtight, polyethylene[1] bladder and a woven polypropylene cover providing the strength of the bag[2]. These polyolefins are readily available and also inexpensive[3]. The problem with the models currently in use arises in the physical handling of two separate bags and the task at hand is therefore to develop a material that combines the functions of the two separate layers currently used for dunnage bags into a single layer, while maintaining the functionality and price competitiveness of existing materials.

The scope of part one was to investigate the materials currently being used to manufacture woven dunnage bags. Material properties that can be tested and used to parameterize these materials had to be identified and thereafter to test a selection of different materials in order to generate an operating envelope for these properties. With the material properties in mind it is necessary to investigate materials that can be used as alternatives to the existing bilayer material. Further development would entail testing of alternative materials and comparing these new materials to the existing material envelope. Recommendations for materials to be tested at prototype level will conclude part one.

1.1.2 Background: Dunnage bags

The main reason for investigating various polyolefins is that they are readily available and inexpensive[4]. An added bonus is that polyolefins are also re-usable and retain their mechanical properties well when recycled[5].

Some of the key characteristics to be tested for a dunnage bag are: tensile strength, permeability and puncture resistance. Knowing this, specific materials can be investigated in the polyolefin range which exhibit these key characteristics. In this range, the materials currently used are low density polyethylene (LDPE) and polypropylene (PP) and will thus be the benchmark for comparison. The aim will therefore be to either match or improve on the properties of currently used commercial materials.

Literature values on specific properties of polymeric materials have been reported by several research groups and are readily available. For permeability literature values, a review of the permeability properties of plastics and elastomers by Liesl K. Massey[6] can be regarded as a good source of permeability characteristics of polyolefins. Air permeability data presented will only be used as a guide to observe different trends from which further study can ensue. These properties of polymers are dependent on many variables; therefore, the tests must be done at similar conditions in order for them to be relatable. Some of these variables include sample preparation, film thickness, and duration of the test as well as temperature at which the test is done[6]. To achieve reproducibility, samples selected must be tested in the same environment to replicate the trends observed. A table of general polymers with their respective air permeability values was set up by Massey[6] (Table 1.1). According to this table poly (ethylene-co-vinyl alcohol) (EVOH) has the best resistance to air permeability. PE and PP can however be found at the other end of the spectrum. This is a general trend found throughout previous studies [6,7].

Table 1.1: Permeability of various polymers[3]

Name	Permeability ($cm^2 \cdot mm/m^2 \cdot day \cdot atm$)[1]
EVOH (dry)	0.008
PVDC	0.1
PAN (70% AN)	0.4
Nylon 6 (dry)	0.4
EVOH (wet)	0.8
PET (oriented)	1
Nylon 6 (wet)	2
Valox PBT	3
PET (not oriented)	3
PVC	4
PETG	6
Ultem PEI	15
Xenoy PBT	18
Noryl PPE	28
Cycolac ABS	39
HDPE	43
PP	59
Lexan PC	92
PPO	742

Mechanical properties have also been extensively studied and documented for example in the book by Landel, R. and Nielsen, L. "Mechanical properties of polymers and composites." (1993)[8] and the book by Osswald, T. A. and Menges, G. "Materials science of polymers for engineers." (1996)[9]. By interpreting the trends reported in these summaries it can be seen that the interplay between strength and ductility of a material is a major factor where either one or the other is favored.

It can be noted from literature that not one single polymer has all the right properties such as a high yield stress, low Young's modulus, high puncture resistance and low air permeability required to make a single layer dunnage bag. A perfect balance of all these properties should be achievable by blending materials with the desired properties. This has been done before in several ways for food packaging barrier materials. An example of such a blend was shown by Ait-Kadi et al.[7] where PP and EVOH were blended with a suitable compatibilizer, resulting in a final product with the barrier properties of EVOH and the mechanical properties of PP. Other

[1]Note the permeability units are different than for this study.

barrier film examples include EVOH blended into a matrix of PE or polyamide[10]. These studies made use of more expensive EVOH and polyamide which are undesirable when material cost is one of the main concerns. Thus polyolefins due to their relative low costs are therefore of main interest in the current study. EVOH is however still included to determine the achievable spectrum of properties possible. The materials are listed below.

1.2 Experimental

1.2.1 Material selection

The selected materials possess a variety of the favorable characteristics required for a dunnage bag, however, none of the individual materials poses all of the favorable characteristics. This wide selection of material characteristics ensures a broad matrix in which various different properties can be related simultaneously.

- LDPE: Low density polyethylene. The most common and widely used polyolefin. The inner bladders of currently used dunnage bags are made of this material. Therefore it should have good resistance to oxygen permeability. As we can see from Table 1.1, however, it is situated at the wrong end of the permeability spectrum.

- iPP: Isotactic polypropylene. This is also a commonly used and strong polyolefin. It is however very rigid which makes it brittle and fails catastrophically when subjected to high loads[11]. This material is currently being used in the woven outer layer of the dunnage bags in order to provide strength.

- CMR348: Impact Polypropylene. This material is a co-polymer provided by Sasol which consists of a reactor blend of polypropylene and ethylene/propylene copolymer. This grade has a 9.4 mol% ethylene co-monomer content. Combining these two materials in a copolymer results in a material with the strength of polypropylene and the flexibility of polyethylene.

- CMR648: Impact Polypropylene. This material is a copolymer provided by Sasol which consists of a reactor blend of polypropylene and ethylene/propylene copolymer. This grade has 18.5 mol% ethylene co-monomer content. The increased ethylene content provides more flexibility compared to CMR348

- EVOH27: Poly (ethylene-co-vinyl alcohol). This copolymer with 27 mol% ethylene content is known for its excellent barrier properties [Table 1.1].

- EVOH44: Poly (ethylene-co-vinyl alcohol) with 44 mol% ethylene content. In order to investigate the effect of extra ethylene a sample with EVOH44 was also tested.

1.2.2 Sample preparation

All of the raw materials (2 g, total weight) were melt-pressed one by one into thin films with a thickness of 200 μm in a pressurized melt press. Samples were pressed between two aluminum blocks covered with Teflon sheets and spaced by a copper shim (200 μm gap) to guarantee constant thickness. Samples were held in position at 10 °C above their respective melting points for 2 minutes under no pressure to allow for sufficient melting. Thereafter the pressure was increased to 200 kPa for 4 minutes and then removed to cool to room temperature (23 °C). The polymer films were cut to the required size for each test that was to follow.

1.2.3 Test methods

1.2.3.1 Permeability testing

A test method for measurement of air permeability of polymer films was developed (for a detailed description of this method see Chapter 4). The method works on the basis of gas mass loss over time through a membrane in a temperature controlled closed system. Definite reproducible trends were seen when comparing the different films. These trends were also in good agreement with those seen in literature[6]. Gas permeability could thus confidently be analyzed.

1.2.3.2 Mechanical testing

Tensile testing (ASTM-D883) and puncture testing (FTMS 101C - Method 2065) was done using a LRX plus series materials testing machine (AMETEK Inc.). For tensile testing the test specimens were cut into dumbbell shapes [Figure 1.1] and then clamped in place using rubber–lined clamps, which prevent the specimen from slipping out upon deformation. A load cell of 5 kN operating at a crosshead speed of 50 mm/min was then used to pull the sample in the machine direction until rupture occurred. For puncture testing, the machine was switched to compression

mode and fitted with a stainless steel puncturing needle with a rounded point measuring 1 mm in diameter. The specimen was cut into a round disc (1cm diameter) and clamped in place. The same load cell and crosshead speed was used as in for tensile testing and the needle was allowed to puncture the specimen in the machine direction.

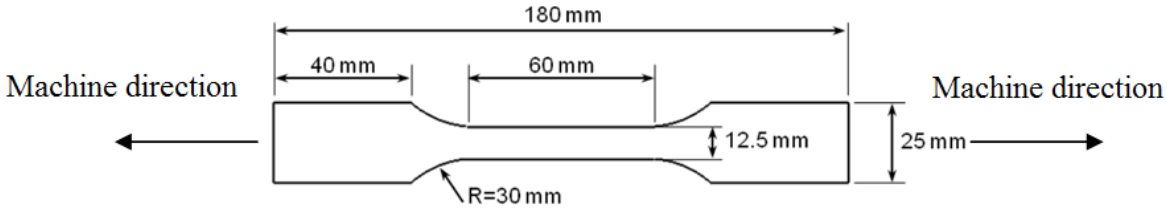

Figure 1.1: Dimension of dumbbell-shaped specimens used for tensile testing.

Both tests were repeated up to five times for each specimen and deemed reproducible, it also yielded results comparable to literature[8]. Tensile tests provided us with yield stress results (the moment at which a material undergoes permanent deformation upon being subjected to an external force) as well as the Young's modulus (initial linear relationship between stress and percentage strain, i.e. stiffness) results. Puncture resistance tests provided us with the bearable load and extension each material can handle before rupture occurred. The type of rupture can also be evaluated visually by inspection of the propagating crack through the material.

1.3 Results and Discussion

1.3.1 Puncture resistance testing.

In Figure 1.2 it can be seen that EVOH27 has the highest puncture resistance and LDPE the lowest. The type of breakage, however, for EVOH (Sample B; Figure 1.3) was catastrophic with the cracks propagating right through the entire material. For LDPE (Sample A; Figure 1.3) on the other hand, no propagating crack formed and the material surrounded the needle neatly. In the case of a dunnage bag the latter behavior will be favorable. It is therefore necessary to try and find a balance between the high stress resistance of EVOH and the flexibility of LDPE. CMR348 failed in a similar manner to LDPE, but it was more resistant to puncturing and therefore seemed to be a more favorable candidate for further investigation.

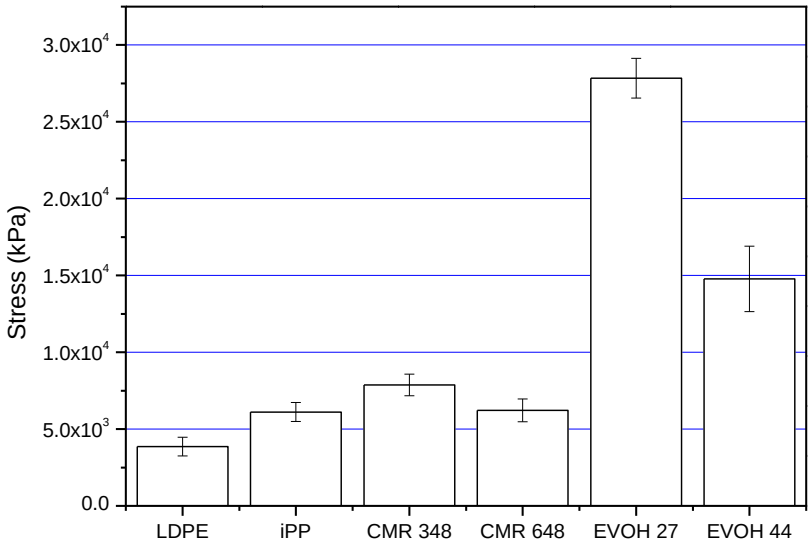

Figure 1.2: Puncture resistance results.

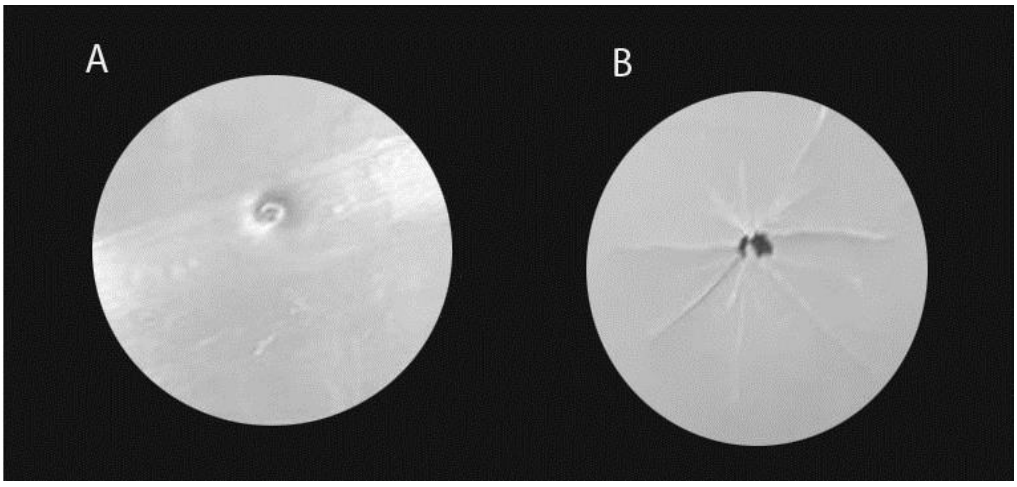

Figure 1.3: Images of puncture test specimens A (LDPE) and B (EVOH 27).

1.3.2 Tensile testing

The trend seen in puncture resistance with respect to EVOH27 and LDPE correlates strongly to the trend seen in the yield stress (onset of permanent deformation) [Figure 1.4]. The visual element of the puncture test however is lost; therefore the Young's modulus is also investigated [Figure 1.5] during tensile testing which relates to the flexibility of the material (this gives an idea of how the material will break). The same trend for breaking which was visually observed through puncture testing was confirmed in the trend we see in the graph of the Young's modulus. EVOH27 showed the highest yield strength as well as Young's modulus with LDPE delivering the lowest values, these two materials thus represents the boundary values of the master curve that was plotted. Both ends of the spectrum are not suitable for the desired end-product as EVOH27 is too rigid and LDPE is too flexible. It was thus necessary to target a material in the between these two extremes. Stress strain curves are presented in Appendix 1.1.

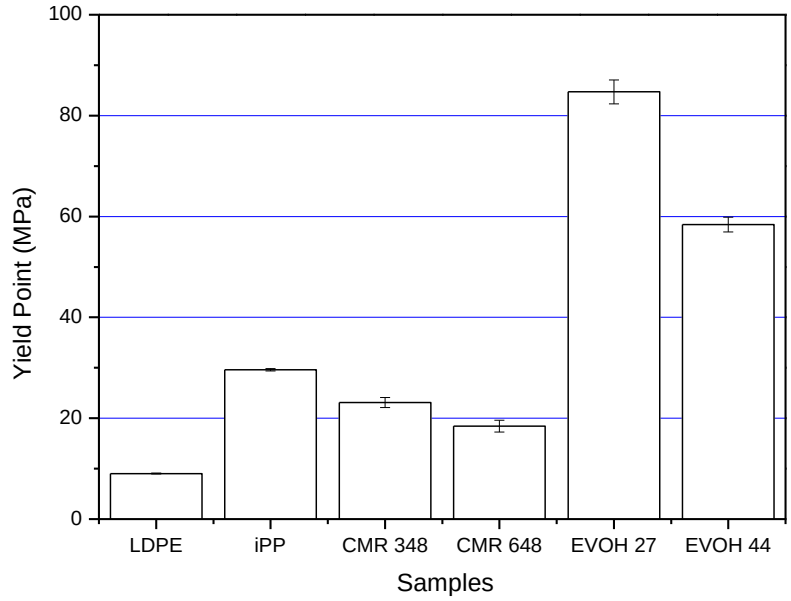

Figure 1.4: Yield stress results.

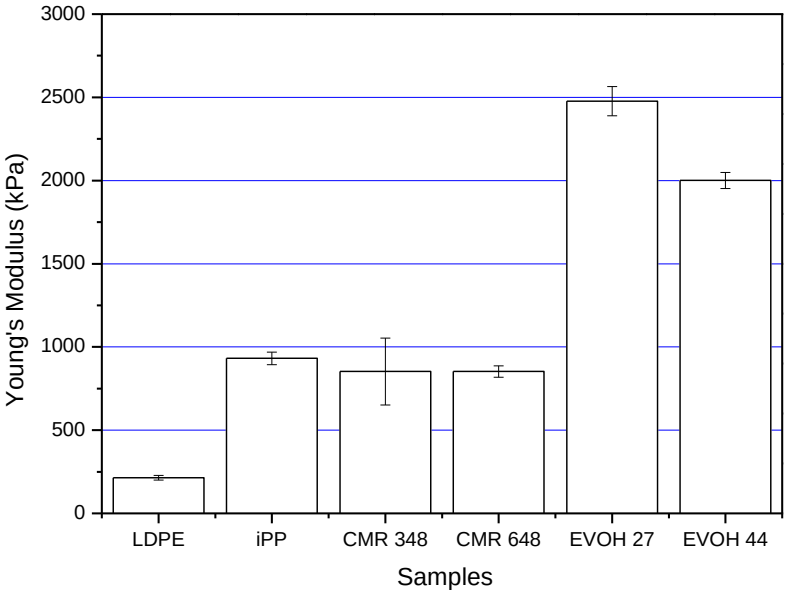

Figure 1.5: Young's modulus results.

1.3.3 Air permeability testing.

Figure 1.6 shows that LDPE had the highest permeability with the EVOH samples having the lowest, indicating the good barrier properties of EVOH. Various parameters could be affecting the permeability of these samples such as percentage crystallinity, crystal structure, fractional free volume or chemical composition. iPP has a comparable permeability to that of EVOH, it is however too rigid for industrial use. LDPE had higher permeability compared to the other materials. CMR348 and CMR648 had different barrier properties with CMR648 having a slightly higher permeability, implying that the amount of ethylene present in the CMR has some effect on the on one of the parameters which influences the permeability.

It was observed that materials performing well in one test, lacked in others and vice versa. Therefore it could be concluded that it is necessary to blend materials of certain beneficial properties in order to create new materials with superior qualities [section 1.4].

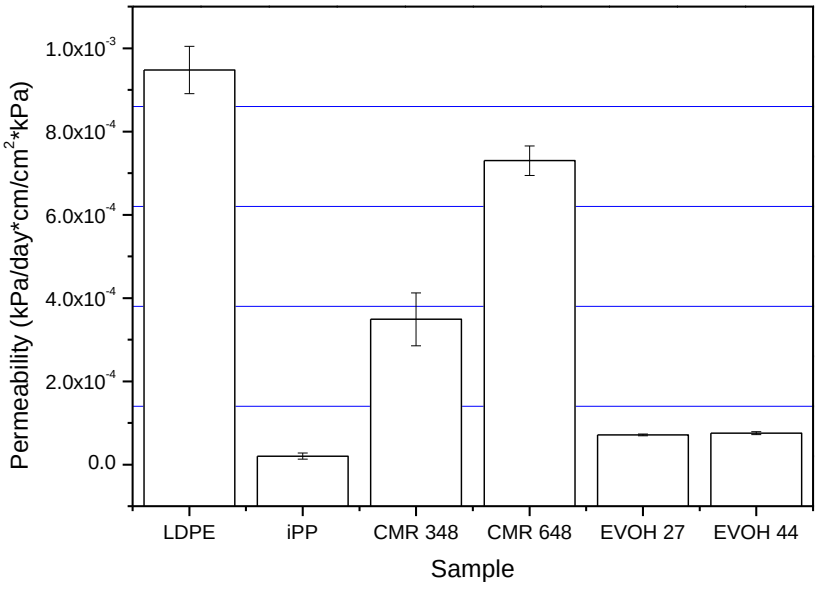

Figure 1.6: Permeability testing results.

1.4 Blending of materials

First a master curve of yield stress versus Young's modulus was constructed. This is illustrated in Figure1.7 which was used to develop the performance envelope. The direction of the arrows on the curve indicates favorable properties. The square on the master curve indicates the targeted area of properties that were to be achieved. Blends were then made and plotted on this curve. Results are shown in Figure 1.8. Seeing that EVOH27 and CMR348 were on either side of the spectrum, blends of these two polymers were attempted. EVOH27 was chosen for its high yield (strength) and low permeability, and CMR348 was chosen for its flexibility and strength. These two materials however are incompatible and it was therefore necessary to add a suitable compatibilizer namely poly(propylene-graft-maleic anhydride) (PP-g-MA) to the blend. This compatabilizer works on the basis of association to the two chemically different films, the apolar PP segment of the grafted copolymer associates with the apolar CMR348 and the polar MA associates with the polar EVOH polar this decreases the interfacial surface tension effectively binding the two layers[12]. All blends were prepared by stacking the individual layers with the compatibilizer as tie layer in a melt press (160 °C; 0.01 kPa). The following blend ratios were tested:

Table 1.2: Blending compositions.

Name_PP-g-MA (wt %)	Polymer	Blend ratio (wt %)
CEC_10	CMR348	33
	EVOH27	33
	CMR348	33
CEC_5	CMR348	33
	EVOH27	33
	CMR348	33
CE_10	CMR348	50
	EVOH27	50

The first two blends were tested to investigate the effect of the compatibilizer. The percentage compatibilizer had a distinct effect on the strength and stiffness of the blends, but as the compatibilizer was not the main focus of the study; it was decided to continue with only the 10%

PP-g-MA blend, as it gave the most uniform blend. Apart from the ternary blends one binary blend was also prepared. Blend compositions are shown in Table 1.2.

It was evident that the binary blend behaved differently to the trilayer blend and the absence of the second EVOH layer, shifted both the yield stress and Young's modulus to higher values. In

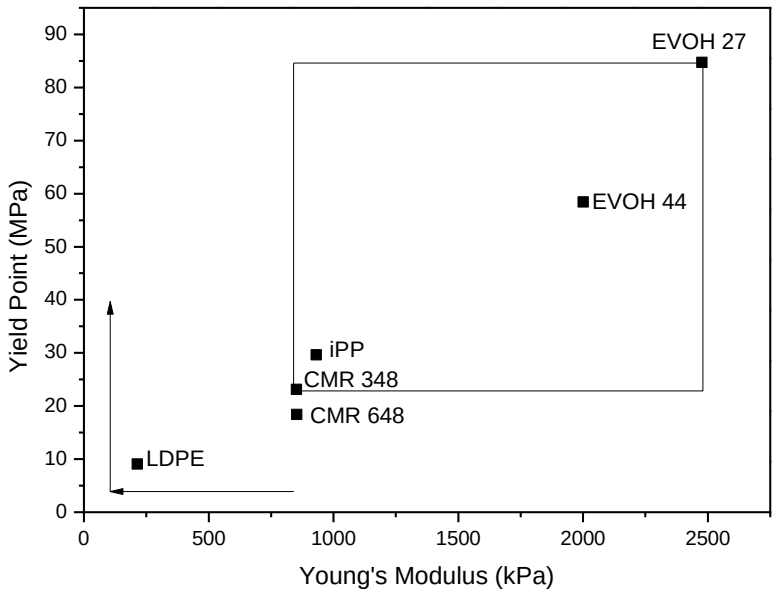

Figure 1.7: Comparison of yield stress versus Young's modulus for neat polymers.

Figure 1.8 it can be seen that by blending the two materials a hybrid material with properties within the targeted range of the master curve could be obtained.

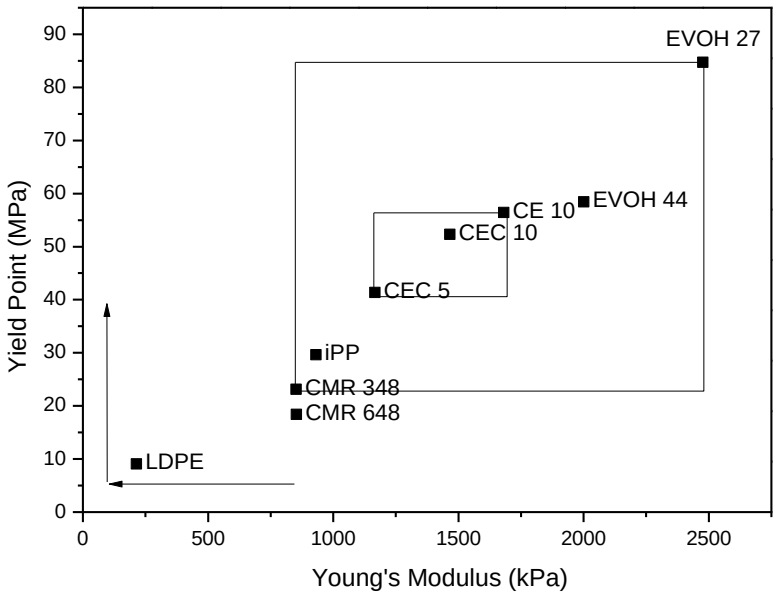

Figure 1.8: Comparison of yield stress versus Young's modulus of neat materials and polymer blends.

Figure 1.9 illustrates the yield stress versus the permeability for neat materials. The block inside the master curve indicates the targeted area of properties that were to be achieved. In Figure 1.10 it can be seen that the permeability decreases for the blends rendering them inconsistent with the desired outcome. This could be due to the added compatibilizer creating areas of higher permeability or processing conditions that are not favorable for blending. While the initial stage of the research, comprising the analysis of various commercially available polymers w.r.t. permeability, puncture resistance and yield strength was successful in terms of fundamental properties, it became clear that the effect of processing conditions when dealing with polymer blends could be a determining factor and thus a restrictive one within the scope of this study. It was therefore decided to focus on two types of material and to investigate effect of the chemical composition and the microstructural morphology and physical properties of these materials.

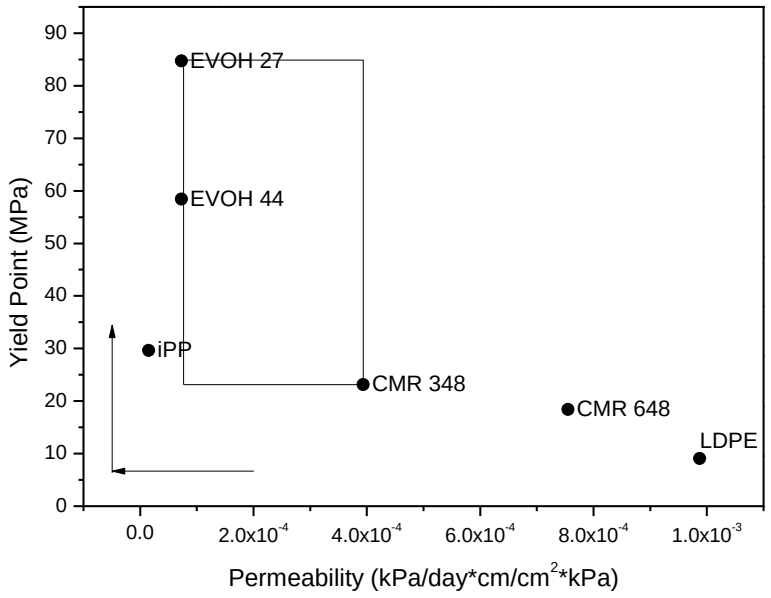

Figure 1.9: Yield stress versus permeability for neat materials.

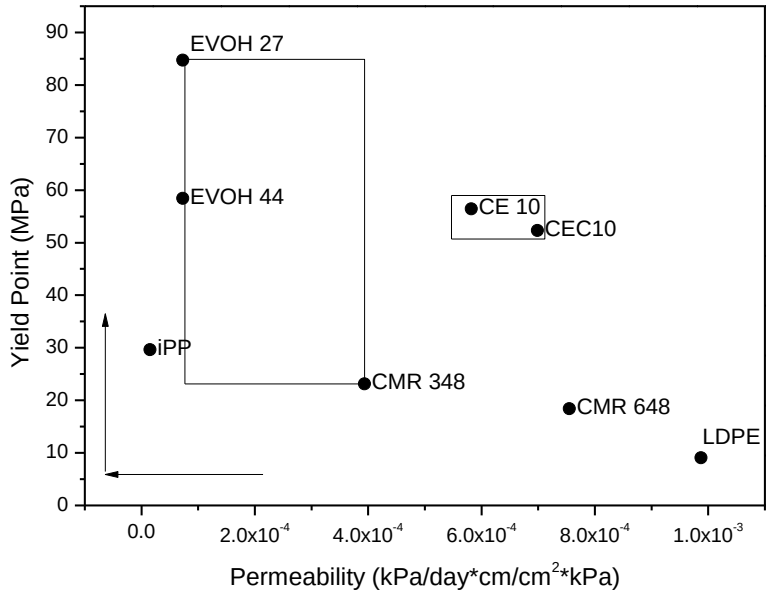

Figure 1.10: Yield stress versus permeability for neat materials and polymer blends.

1.5 Part one: Conclusion

All test methods yielded accurate, insightful and reproducible results. The materials selected comprise of a wide range of selected properties allowing for a better understanding of the fundamentals needed for the desired end use.

From the permeability experiment distinguishable difference within the sample set could be observed. LDPE which is currently being used as the impermeable layer in the double layer dunnage bag showed the highest permeability. EVOH27 on the other hand exhibited the best gas barrier properties. From the mechanical testing experiments however EVOH had a high rigidity which caused it to fail catastrophically. when examining the master curves, it was observed that CMR348 was a more favorable candidate due to its greater flexibility.

A series of blends were made with the aim of combining the optimal barrier properties of EVOH27 with favorable mechanical properties of CMR348. This targeted area of favorable properties could be achieved in the mechanical experiments, but the permeability testing proved to be a lot more difficult than was expected. The reason for this was concluded to be due to the incompatibility of the two materials and the major role which the compatibilizer (PP-g-MA) played, it resulted in lower permeability properties than the initial materials had before blending. No further investigation into the blends, were done due to the numerous effects the compatibilizer had on it. To eliminate these effects, part two of the study was based on commercially available material and rather trying to investigate the processing conditions thereof to manipulate the grade of material in favor of the desired application.

Further expansion of the envelope as well as testing of different material combinations within it should help reach the goal of creating a single layer dunnage bag material with similar or even superior properties to those currently in use. During this stage of the study there was also a focus shift away from the application of dunnage bags. It was decided to migrate towards a more fundamental study of the crystal morphology and the effects thereof on permeability. This data could then be used in a broader application base such as food packaging.

Impact polypropylene was identified for further study. CMR348 does lack resistance to permeability and ethylene content seems to be the main cause of this deficiency to some degree.

The effect of incorporating ethylene into the copolymer should be further investigated. Part two of this study made use of an impact copolymer or heterophasic ethylene-propylene copolymer from Sasol which also had similar ethylene content to that of CMR 348. In this sample set the ethylene content is varied in order to investigate the effect thereof on the permeability properties.

1.6 References

1. Vasile, C. and Pascu, M. *Practical guide to polyethylene*. Shrewsbury (iSmithers Rapra Publishing, , (2005).

2. Maier, C. and Calafut, T. *Polypropylene : the definitive user's guide and databook*. New York (Plastics Design Library, 1998).

3. Galiè, F. Global Market Trends and Investments in Polyethylene and Polypropylene. *Icis* **,** 1–3 (2016).

4. Mohanty, A. D. and Bae, C. Transition Metal-Catalyzed Functionalization of Polyolefins Containing CC, CC, and CH Bonds. in *Advances in Organometallic Chemistry* **64,** 1–39 (Elsevier Ltd, 2015).

5. Luijsterburg, B. and Goossens, H. Assessment of plastic packaging waste: Material origin, methods, properties. *Resour. Conserv. Recycl.* **85,** 88–97 (2014).

6. Massey, L. K. *Permeability Properties of Plastics and Elastomers*. (Plastics Design Library, New York, (2003).

7. Ait-Kadi, A., Bousmina, M., Yousefi, A. A. and Mighri, F. High performance structured polymer barrier films obtained from compatibilized polypropylene/ethylene vinyl alcohol blends. *Polym. Eng. Sci.* **47,** 1114–1121 (2007).

8. Landel, R. and Nielsen, L. *Mechanical properties of polymers and composites*. New York (M. Dekker, 1993).

9. Osswald, T. A. and Menges, G. *Materials science of polymers for engineers*. New York (Hanser, 1996).

10. Lange, J. and Yves, W. Recent innovations in barrier technologies for plastic packaging - a review. *Packag. Technol. Sci.* **16,** 149–158 (2003).

11. Nielsen, L. E. and Landel, R. F. *Mechanical properties of polymers and composites*. New York (M. Dekker, 1994).

12. Kim, J. K., Kim, S. and Park, C. E. Compatibilization mechanism of polymer blends with an in-situ compatibilizer. *Polymer (Guildf).* **38,** 2155–2164 (1997).

Part II: Morphological effects of ethylene incorporation on heterophasic ethylene-propylene copolymer (HEPC) films.

Chapter 2

2.1 Introduction

Since the introduction of highly crystalline polypropylene (PP) in 1955[1] it has been one of the most widely used and important polyolefins in the world. It is estimated that by the year 2020 PP will be at a demand of up to 62.4 million Tonnes p.a.[2]. PP is a dynamic polymer with attractive properties such as excellent processability, heat and chemical resistance. These properties combined with its low specific gravity and low cost, make it an extremely desirable commodity in various industries. Some of these industries include the automotive, textiles, medical and food packaging industries[2-3].

When focusing on the physical properties such as tensile and impact strength, PP homopolymer however, does have some inherent unfavorable qualities such as its brittleness and low impact strength. This led to the development of a new hybrid class of materials where the combination of different properties of polymers results in a new material possessing superior qualities when compared to the constituent homopolymers[4]. Polyolefins similar to PP such as polyethylene (PE), exhibiting superior properties to that of PP, can be incorporated into PP in different ways[4]. The incorporation of different α-olefins into polypropylene is done by blending or copolymerisation[5]. Shell oil company was the first to patent modified polyolefins by homopolymerizing of PP and then subsequently incorporating in-reactor ethylene-propylene copolymer prepared in-reactor and thus creating high impact strength PP[6].

A very popular class of materials currently being used is impact copolymers or heterophasic ethylene propylene copolymers (HEPCs). It has extremely high strength and impact properties, thus a fundamental understanding of the behaviour on a molecular level of these copolymers are essential to allow for tailoring of macroscopic properties and performance.

In part two the aim was to relate macroscopic properties with the molecular behaviour and morphology of polymer films with varying molecular characteristics. A variety of test methods were utilized to relate the macroscopic property of air permeability with the polymer's microscopic morphology i.e. crystallinity, crystal structure and fractional free volume.

2.2 Background

2.1.1 Polypropylene: An overview

Highly crystalline polypropylene was first introduced by Giulio Natta in 1955[1] using $TiCl_3$ as the catalyst and $AlEt_2Cl$ as the cocatalyst. This was achieved by expanding on the work done by Karl Ziegler and his Aufbau reaction for the polymerisation of polyethylene[7]. Since then the catalyst and manufacturing technologies have greatly improved to make polypropylene which is one of the most utilized polymers in the world, second only to polyethylene[8].

Three different forms of PP homopolymer [Figure 2.1] can be made, namely isotactic, syndiotactic and atactic polypropylene, with the isotactic form being the most utilized. Isotactic PP consists of high stereoregularity which enables close packing of the molecular chains, thus creating a highly crystalline material[9].

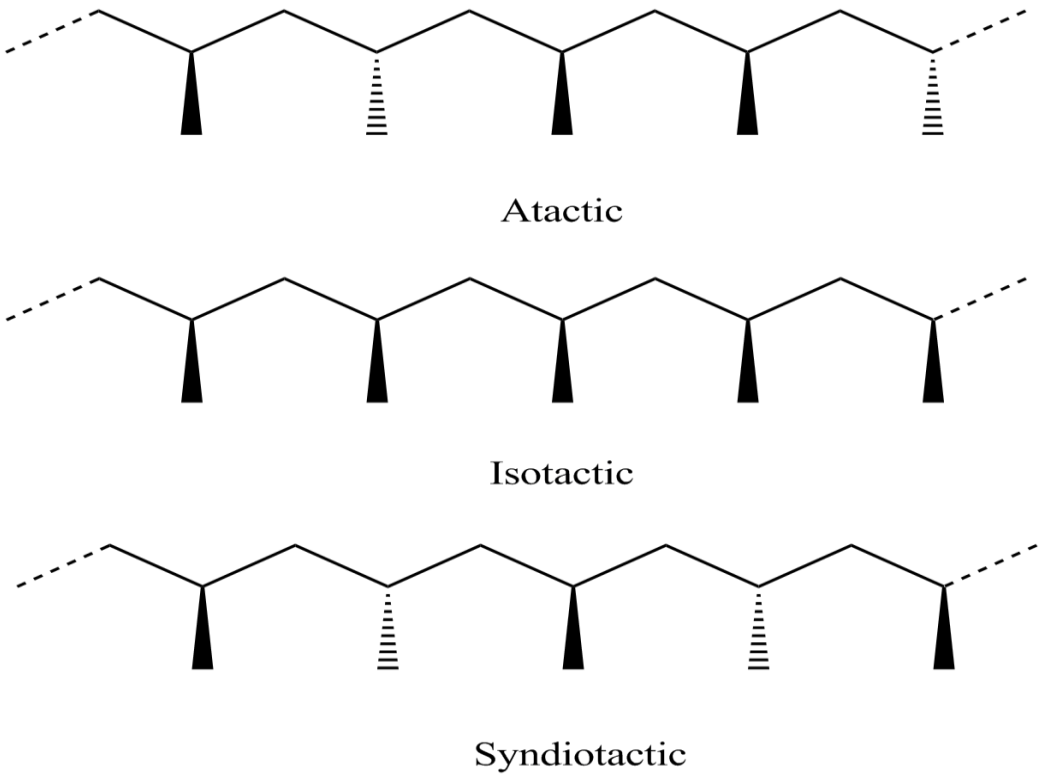

Figure 2.1: Tacticity of polypropylene.

Today the Novolen® process described schematically in Figure 2.2 below is one of the more effective commercial routes for synthesizing PP[8]. This process only makes use of gas phase polymerisation in which a Ziegler-Nata catalyst and stereomodifier is used[4]. Monomers are fed into one or both reactors. Controlling of molecular weight is achieved by the introduction of Hydrogen. Temperature, pressure and monomer concentrations are adjusted to the specific grade that is to be produced[10].

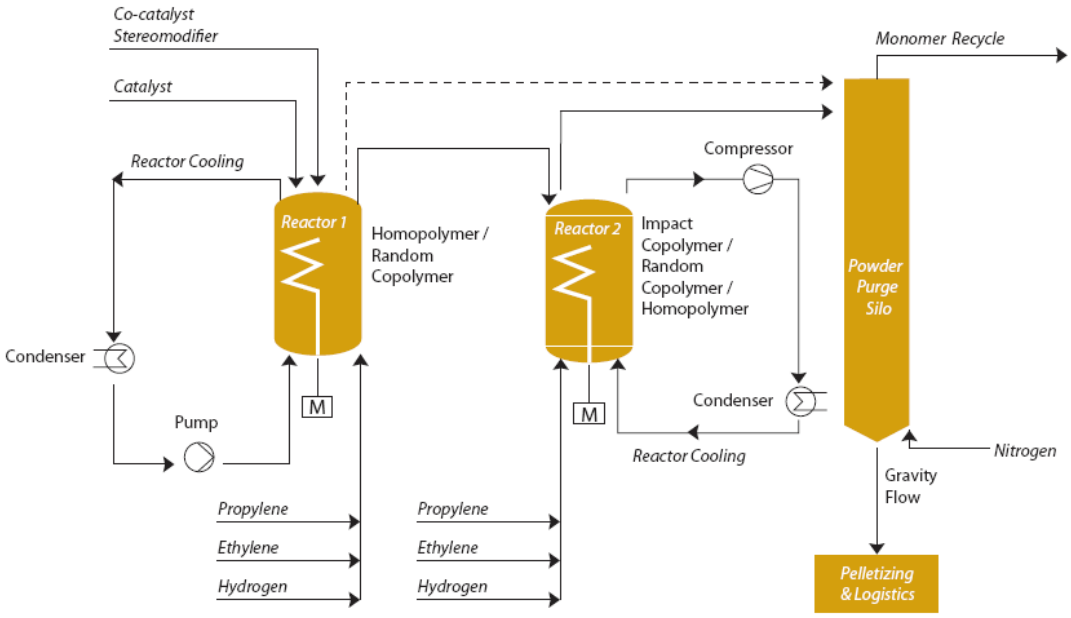

Figure 2.2: Novolen process[10]

Polypropylene is a very rigid polymer and is therefore highly brittle at low temperatures which makes it ineffective in some applications[11]. Industrial demand arose for a low cost recyclable material of the same tenacity as PP, but with better impact resistance especially at low temperatures led to the incorporation of ethylene comonomer, which has great impact properties. Within this process only one or even both reactors can be utilised depending on the type of polymer to be produced. This second monomer can be introduced in the first reactor to create random copolymer or in the second reactor to create heterophasic ethylene propylene copolymers (HEPCs).

2.1.2 Random copolymers

This form of ethylene incorporation is done by introducing the two monomers, ethylene and propylene in the same reactor with a heterogeneous catalyst[12]. Various factors such as the stereo specific nature of the catalyst, reaction conditions and the reactivity ratios of the monomers are responsible for the degree and type of copolymerisation achieved[4] [Figure 2.3] .

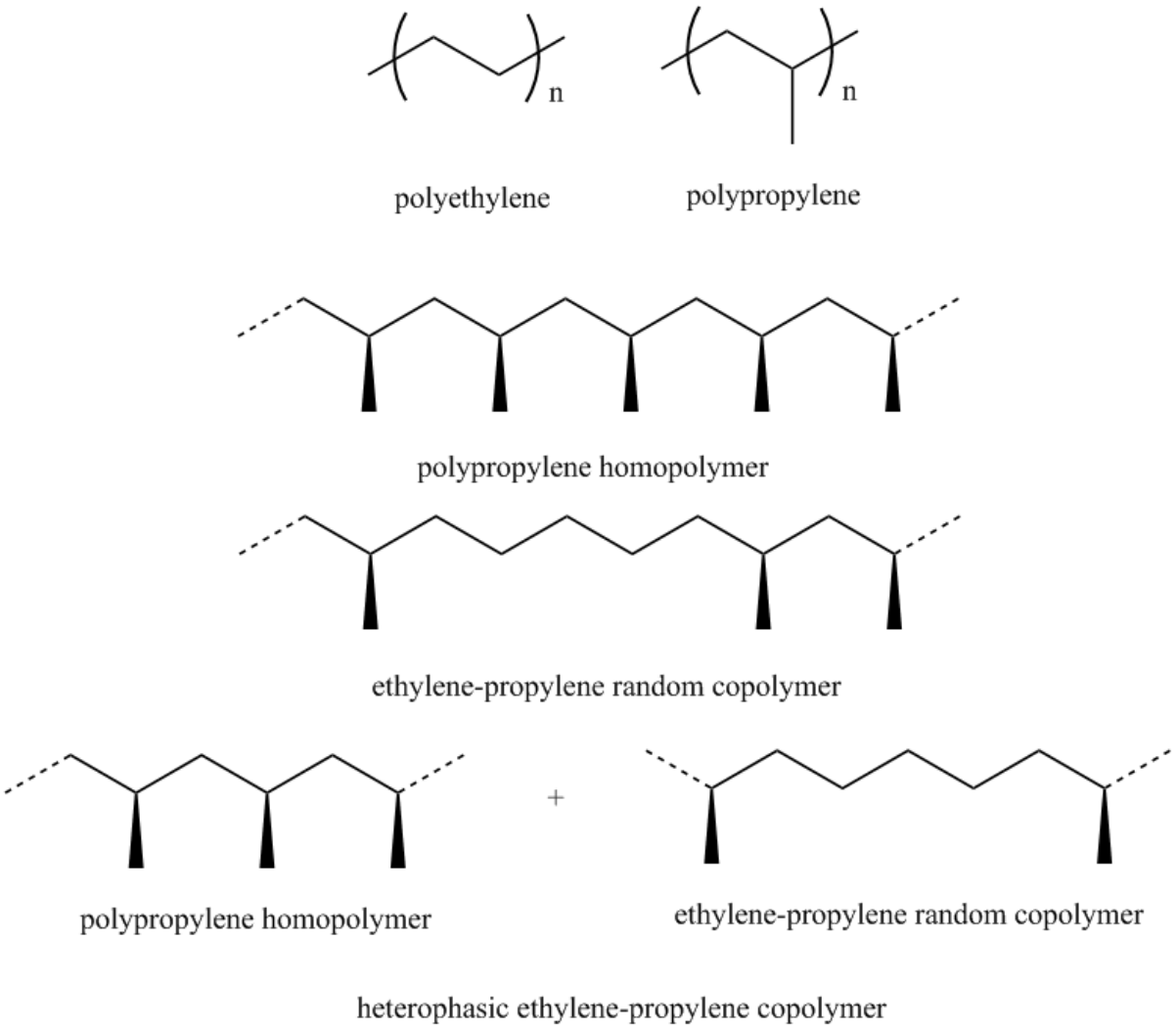

Figure 2.3: Heterophasic ethylene propylene copolymer.

2.1.3 Heterophasic ethylene propylene copolymers (HEPCs).

Polymerisation of HEPCs [Figure 2.3] is achieved via a two-stage reactor setup. Two reactors [Figure 2.2] are set up in series, in the first reactor only isotactic PP is produced. Homopolymer then passes to the second reactor where a mixture of ethylene and propylene monomers are introduced to produce a random copolymer which is incorporated in and around the homopolymer. Throughout the reaction hydrogen is included in the mixture to act as a terminating agent for molecular weight control[8]. This process results in a ternary mixture of PP

homopolymer ethylene-propylene rubber and some ethylene propylene semi-crystalline material[3].

2.3 Morphology

2.3.1 Permeability

Studying a macroscopic property such as the permeability of polymers is important for downstream purposes, but this property must be related to the microstructure to get a better understanding of how these parameters affect each other. A polymeric film is said to be air permeable if it allows an air molecule to pass through it.

Transport of gases are dependent on the following occurrences:

- adsorption onto the polymer surface
- absorption into the polymer
- diffusion through the polymer matrix
- desorption through the polymer wall and
- evaporation off the polymer surface[13].

Permeability is measured by tracking the gas mass loss through a membrane of certain dimensions over a period of one day via the following equation and at standard conditions[14].

$$\frac{\Delta \mathbf{mgas}}{\Delta \mathbf{t}} = \boldsymbol{P}\frac{\boldsymbol{A}\Delta \mathbf{p}}{\boldsymbol{l}} \qquad \textbf{Equation 1.1}$$

Where:

- P = permeability of barrier
- Δm gas / Δt = transmission rate
- A = area of barrier
- l = thickness of barrier
- Δp = partial pressure difference across the barrier

By rearranging the equation the formula for permeability is obtained:

$$P = \frac{\Delta m \cdot gas \cdot l}{\Delta t \cdot A \cdot \Delta p} \qquad \textbf{Equation 1.2}$$

The units for permeability at standard conditions are:

$$\left[\frac{cm^3 \cdot mm}{m^2 \cdot day \cdot atm}\right]$$

Various factors affect permeability in polymers. Specific characteristics of a polymer, for example the chemical composition and physical state, the type of penetrating gas as well as the environment the sample is tested in, all play a major role in the permeability of the polymer.[15] Chemical composition, such as functional groups or polarity of a molecular chain may associate and interact with the penetrant causing a delay or enhancement in a gas molecule's diffusion time. Chain mobility which is affected by the temperature and degree of branching or cross-linking contribute to how easily a penetrant can push its way past a chain and diffuse through the material.[16]

Factors that can be controlled such as temperature, pressure, humidity and sample thickness are kept constant in order to eliminate all their respective effects. Samples to be tested are also similar in molecular makeup (apolar polyolefins) and sourced from the same producer to eliminate any processing differences. A penetrant cannot diffuse through a crystallite and needs enough amorphous region in order to be able to diffuse through a material[14], it was therefore necessary to probe the crystallinity of the materials.

2.3.2 Crystallinity and crystal forms as determined by X-ray diffraction (XRD).

Crystallinity in PP homopolymers is dependent inter alia, on the tacticity of the molecules. As previously mentioned [2.1.1] a highly isotactic polypropylene (iPP) will result in a higher crystallinity which is a result of low steric hindrance between the methyl side groups which allows molecules coming into sufficient proximity and form strong intermolecular bonds and sufficient crystal packing[17].

Crystal structures of PP typically consists of a 3_1 helical structure [Figure 2.4][18] in either a left handed up/down or right handed up/down conformation. These helices adopt an α, β or γ allomorph [Figure 2.5][18]. Three WAXS diffractograms can be seen below, in each case a different sample exhibiting different crystal phases are shown. Defects of the crystal structure are associated with β or γ forms which can be induced through the incorporation of a nucleating agent[19], a comonomer, stress or heat[9]. These phases can be seen in the second and third diffractograms. Next to them is an example of the proposed different Helices' conformation.

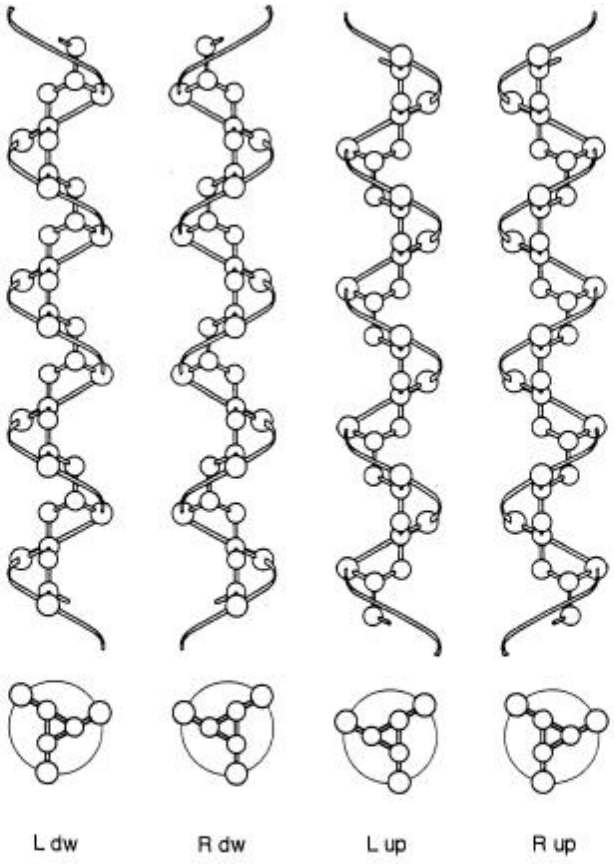

Figure 2.4: Polypropylene helical structure[9].

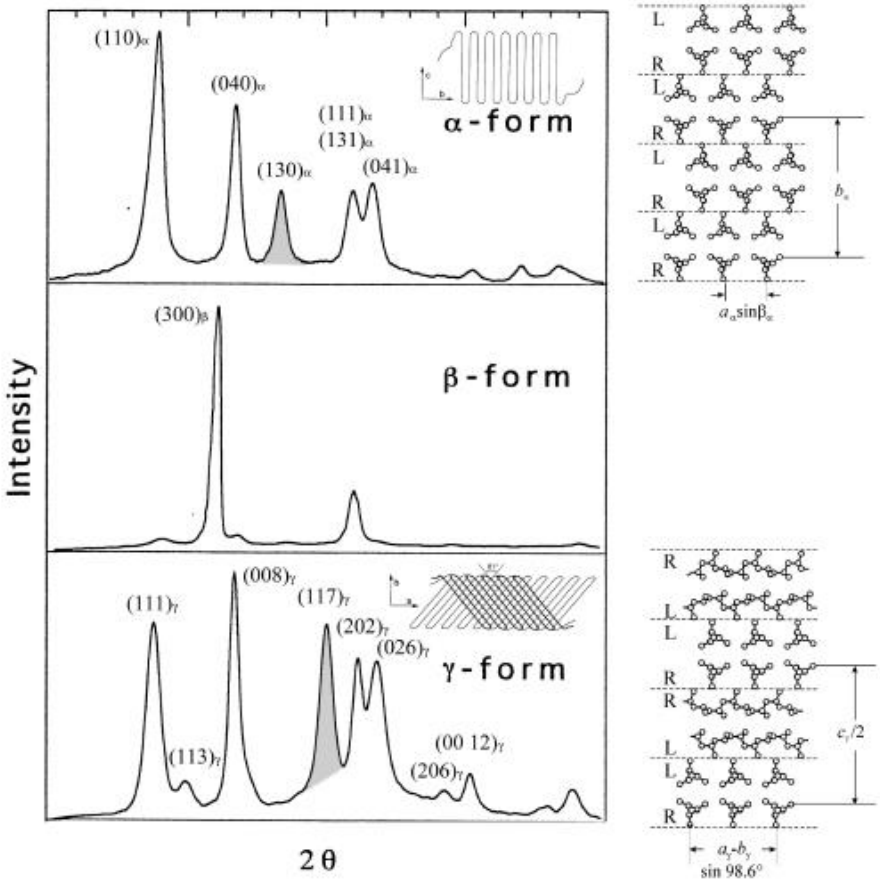

Figure 2.5: Polymorphism in polypropylene X-ray scattering patterns.[9]

2.3.3 The concept of fractional free volume.

Free volume was first introduced in order to explain elastomeric behaviour in which the general concept is that in order for a molecule to be displaced there needs to exist sufficient free space for it to move into[20]. Fractional free volume (FFV) is therefore defined as the unoccupied space within a solid material[21], the equation follows:

$$\mathbf{FFV} = \frac{\mathbf{V}-\mathbf{V_0}}{\mathbf{V}} \qquad \textbf{Equation 1.3}$$

Where:

- V = Volume of the material
- V_0 = Volume occupied by the polymeric chains*

*This variable involves various assumptions to be made in approximating its value[21].

Determination of FFV through positron annihilation lifetime spectroscopy (PALS) is one of the best techniques available today[22]. Free volume can be probed through irradiating a polymeric sample with positrons. Positrons are ejected from a decaying radioactive source such as Na^{22}, they consist of the same mass as an electron but exhibit a positive charge. When positrons and electrons combine they can self-annihilate or form a neutral positronium (Ps) atom. These Ps atoms exists in electron deficient open spaces such as the free volume of polymers. These Ps atoms can then undergo "pick–off" annihilation when an electron rich molecule is encountered. Annihilation can take place via parallel or anti-parallel spin combinations creating ortho-Ps (o-Ps) or para-Ps (p-Ps), respectively. O-Ps has a longer lifetime than p-Ps which makes it ideal for studying the free volume of polymers. The annihilation event releases photons in the form of γ-radiation which can then accurately be measured[23]. O-Ps lifetime is a direct correlation of the size and concentration of free volume holes[24].

Having an idea of the trend in the FFV of a series of polymers one can predict/correlate the permeability of the materials for a given diffusant, knowing that free volume theory predicts a linear relationship between log P and 1/FFV[25].

Low permeability will arise from the close packing of molecules leading to a high density and therefore a low FFV[14]. Fractional free volume is also closely associated to the amorphous region of a polymer and therefore, the glass transition temperature of a polymer[20]. As a polymer's temperature is decreased the FFV also decreases until it reaches a lower critical limit and the polymer resembles a glassy state.[20,15]

2.3.4 Polarized-light optical microscopy (POM).

When polymeric materials crystallize into spherulites, they exhibit a property called birefringence (scattering of polarized light in different directions due to different refractive

indices throughout a crystal) which can be monitored on a light microscope through bifocal cross-polarized lenses. This technique enables the user to observe crystal forms and allomorphs[26] such as the Maltese cross in PP spherulites as well as crystal growth allowing for crystal kinetics to be monitored and analyzed. Spherulites can also viewed in high definition which enables a visual analysis on the crystal quality.

2.4 Aims

The aims of part two are:

- Determine the permeability of four different HEPC films.
- Determine the effect of co-monomer inclusion on permeability.
- Determine the effect of morphology on permeability.
- To conclude which analytical techniques best predict the effect of morphology on a polymer film's permeability.
- Apply a set of techniques on different polymer systems to substantiate findings.

2.5 References

1. Natta, G., Pino, P., Corradini, P., Danusso, F., Mantica, E., Mazzanti, G. and Moraglio, G. Crystalline High Polymers of A-Olefins. *J. Am. Chem. Soc.* **77,** 1708–1710 (1955).

2. Rübsam, K., Stomps, B., Böker, A., Jakob, F. and Schwaneberg, U. Anchor peptides: A green and versatile method for polypropylene functionalization. *Polymer (Guildf).* **116,** 124–132 (2017).

3. Magagula, S. and Van Reenen, A. The effect of organic peroxides on the molecular composition of heterophasic ethylene-propylene impact copolymers (HECOs). *MSc Thesis Stellenbosch Univ.* (2015).

4. Harding, G. The fractionation and characterisation of propylene-ethylene random copolymers. *MSc Thesis Stellenbosch Univ.* (2005).

5. Agarwal, V., Van Erp, T. B., Balzano, L., Gahleitner, M., Parkinson, M., Govaert, L. E., Litvinov, V. and Kentgens, A. P. M. The chemical structure of the amorphous phase of propylene-ethylene random copolymers in relation to their stress-strain properties. *Polym. (United Kingdom)* **55,** 896–905 (2014).

6. Short, G. A. (1967) United states patent office No. 3318976, New York, United states: United states patent office.

7. Goodall, B. History and Current State of the Art of PP Polymerization Catalysts. *Journal of Chemical Education* ***6,*** *125-126* (1986).

8. Botha, L. and Van Reenen, A. J. The effect of in-process ethylene incorporation on the evolution of particle morphology and molecular characteristics of commercial heterophasic ethylene propylene copolymers (HEPCs). *Eur. Polym. J.* **49,** 2202–2213 (2013).

9. Van Der Burgt, F.P.T.J. Crystallization of isotactic polypropylene : the influence of stereo-defects. PhD Thesis Technische Universiteit Einhoven (2002).

10. Polypropylene. Available at: https://www.cbi.com/getattachment/a50c26ce-df7a-4268-8ee1-f806af21648c/Polypropylene.aspx. (Accessed: 30th November 2017)

11. Liang, J. Z. and Li, R. K. Y. Rubber toughening in polypropylene: A review. *J. Appl. Polym. Sci.* **77,** 409–417 (2000).

12. Du, Z., Xu, J., Wang, X. and Fan, Z. Microstructure of Ethylene/Propylene Random Copolymers Prepared by a Fluorinated Bis(phenoxy-imine)Ti Catalyst. *Polym. Bull.* **58,** 903–911 (2007).

13. Mark, H. *Encyclopedia of polymer science and technology, concise*. (Wiley, Pittsburg 2013).

14. Massey, L. K. *Permeability Properties of Plastics and Elastomers*. (Plastics Design Library, New York, 2003).

15. Mrkic, S., Galic, K. and Ivankovic, M. Effect of Temperature and Mechanical Stress on Barrier Properties of Polymeric Films Used for Food Packaging. *J. Plast. Film Sheeting* **23,** 239–256 (2007).

16. Lange, J. and Yves, W. Recent innovations in barrier technologies for plastic packaging - a review. *Packag. Technol. Sci.* **16,** 149–158 (2003).

17. Soares, J. B. P. and McKenna, T. F. L. Introduction to Polyolefins. *Polyolefin React. Eng.* ***1***. 1-14 (2012).

18. Salamone, J. *Concise polymeric materials encyclopedia*. Massachusettes, Lowell (1998).

19. Motsoeneng, T. S., Luyt, A. S. and Van Reenen, A. J. Investigation of the crystalline phase morphology of a β-nucleated impact polypropylene copolymer. *J. Appl. Polym. Sci.* **131,** 1–9 (2014).

20. White, R. P. and Lipson, J. E. G. Polymer Free Volume and Its Connection to the Glass Transition. *Macromolecules* **49,** 3987–4007 (2016).

21. Park, J. Y. and Paul, D. R. Correlation and prediction of gas permeability in glassy polymer membrane materials via a modified free volume based group contribution

method. *J. Memb. Sci.* **125,** 23–39 (1997).

22. Bébin, P. and Prud'Homme, R. E. Effect of comp drif. *J. Polym. Sci. Part B Polym. Phys.* **39,** 2363–2377 (2001).

23. Basson, N. Free volume of electrospun organic-inorganic copolymers. *MSc Thesis Stellenbosch Univ.* (2014).

24. Jean, Y. C., Mallon, P. E. and Schrader, D. M. *Principles and applications of positron and positronium chemistry*. World scientific. (2003)

25. Thran, A., Kroll, C. and Faupel, F. Correlation between fractional free volume and diffusivity of gas molecules in glassy polymers. *J. Polym. Sci. Part B Polym. Phys.* **37,** 3344–3358 (1999).

26. Crist, B. and Schultz, J. M. Polymer spherulites: A critical review. *Prog. Polym. Sci.* **56,** 1–63 (2016).

Chapter 3:

3.1 Sample production and selection

3.1.1 Sample production

Samples of HEPCs were obtained from Sasol Polymers' Polymer technology services centre. The samples were produced via the commercial Novolen® [Figure 2.2] gas phase process. The setup is comprised of two reactors in series. In the first reactor a Ziegler-Natta catalyst, a silane compound for stereo control and an aluminum alkyl for catalyst activation and poison scavenging are added. This produces a PP homopolymer which is then transferred to the second reactor. In the second reactor ethylene as well as more propylene monomer is introduced for copolymerization to commence. Time spent in the second reactor is related to ethylene incorporation into the copolymer.

3.1.2 Sample selection

Samples were extracted from the second reactor (in powder form) at different intervals starting at T_0 (0 minutes), T_30 (30 minutes) etc. and thus consists of varying amounts of ethylene inclusion. Infrared spectroscopy was used to determine the ethylene content of each sample[2]. Four samples were chosen to represent the entire range as accurately as possible [Table 3.1].

Table 3.1: Sample selection.

Name_(min)	Ethylene content (mol %)
T_0	0
T_30	2
T_90	6.8
T_150	9.3

3.1.3 Sample preparation

Nascent polymer powder (2 g) were mixed with heat stabilizers Irganox 1010 and Irgafos 168, (2 wt %) and melt-pressed into thin films with a thickness of about 200 μm. Using two aluminum blocks covered with Teflon sheets and a shim (200 μm) to guarantee constant thickness, the

samples were held in position at 180 °C for 2 minutes under no pressure. After sufficient melting the pressure was increased to 200 kPa for 4 minutes and then removed to cool to room temperature (23 °C). Thereafter specimens were cut to the required size for each test that was to follow.

3.2 Experimental

3.2.1 Permeability testing

Testing was done using an in-house method. A sealable stainless steel chamber fitted with a pressure gauge (0-250 kPa) was used to clamp down the melt-pressed films [Figure 3.1]. At the inlet, the film was pressurized (250 kPa) with oxygen and tightly sealed. The instrument was then placed in a temperature controlled oven (23 °C, 40 % RH, 24h) where the pressure drop was monitored hourly over a period of 24 hours. Experiments were repeated up to 3 times. In the developing stage of the experiment, the instrument was calibrated using an impermeable glass disc, the disc was inserted as a specimen and a constant error was observed and accounted for in the subsequent experiments results of this are shown in Appendix 2.1.

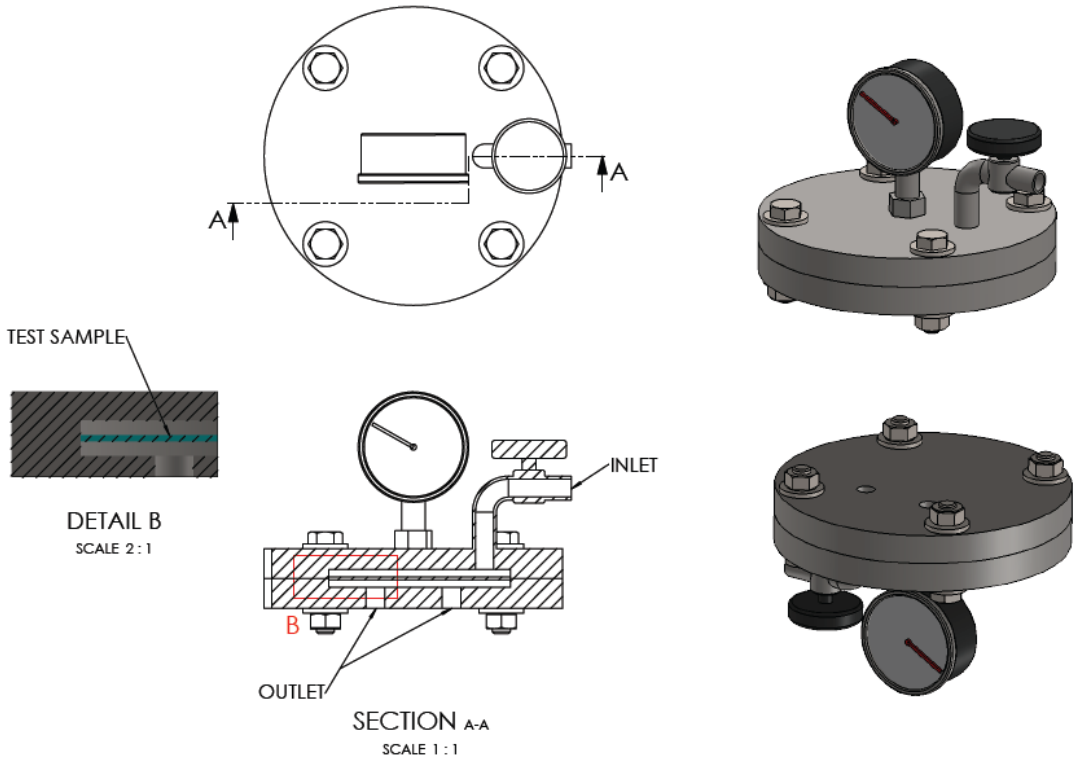

Figure 3.1: Permeability testing instrument.

3.2.2 Differential scanning calorimetry (DSC)

3.2.2.1 Conventional DSC

Melting and crystallization behavior of the polymer samples were analyzed by means of a TA instruments Q100 differential calorimeter, calibrated with Indium metal according to standard procedures. A three-step cycle was implemented wherein each polymer sample (4 mg) was weighed and heated from room temperature to 200 °C in the first cycle at a heating rate of 10°C·min^{-1}, this is done to remove any thermal history of the samples. Samples were kept isothermally at 200 °C for 3 minutes, after which they were cooled to 25 °C at 10 °C·min^{-1}. During the final step the temperature was kept constant at 25 °C for 3 minutes and then heated to 200 °C. Only data obtained from the second heating cycle was processed for all the thermal analysis calculations. In all the DSC thermograms, the exothermic transitions were associated

with the upwards curves while the endothermic transitions were associated with the downwards curves. The DSC measurements were carried out in an inert nitrogen atmosphere at a purge gas flow rate of 20 ml·min^{-1}. Data was analyzed using TA universal analysis software.

3.2.2.2 Successive self-nucleation and annealing (SSA)

This technique was implemented as a fractionation method to investigate the crystal heterogeneity. The only difference from classical DSC was in the cycling program method. This technique was conducted using 11 cycles instead of 3. The first two cycles were similar as in classical DSC. Thereafter each heating step was done to exactly 5 °C lower than that of the previous heating step. This left the higher melting point crystals intact thus separating the polymers based on their crystallizability. The final heating cycle was done up to 200 °C and resulted in multiple melting endotherms correlating to the different crystallizable domains. Data was analyzed using TA universal analysis software.

3.2.3 X-ray diffraction (XRD)

X-ray diffraction data was collected using a Bruker D2 PHASER diffractometer equipped with a Lynxeye 1D detector and Ni-filtered Cu Kα radiation (λ = 1.5418 Å; 30 kV, 10 mA generator parameters; restricted by a 1.0 mm divergence slit and a 2.5 Soller collimator). Samples were loaded onto a zero-background holder and patterns were recorded in the 2θ range from 5°−35° with a step size of 0.02° and step time of 1s. Melt-pressed samples were used as is and powder samples were first melted in DSC pans to also form thin films. All experiments were done at ambient conditions. The data was analyzed using OriginPro v. 8.5 software. All crystalline peaks were de-convoluted, separated from the amorphous halo and integrated.

3.2.4 Positron annihilation lifetime spectroscopy (PALS)

All PALS measurements were carried out at room temperature using a standard fast-fast coincidence system with a timing resolution of 250 ps. The positron source used was radioactive ^{22}Na in the form of NaCl which was deposited on thin Kapton foil. All polymer samples were pressed into films of 2-3 mm thick. The radioactive source was deposited and sandwiched between two pressed films of polymer and then encapsulated with aluminum foil. Thereafter it was placed between two photomultiplier detectors which were placed at 180º to

each other and at least 1cm apart to minimize backscattering. The duration of the measurements lasted until a minimum of $1x10^6$ counts were collected (30-60 minutes). Positron lifetime spectra were collected for each sample and evaluated with PATFIT[1] software. Lifetime and intensity values were extracted from the spectra with a model function consisting of a sum of decaying exponentials convoluted with the resolution function of the lifetime spectrometer plus a constant background.

3.2.5 Polarized-light optical microscope (POM)

To investigate the crystal growth rate and morphology an Olympus CX-31 microscope was used equipped with two polarized lenses and a heating stage from Pike technologies. Nascent samples were placed in-between two glass slides and melted to a thickness of about 20µm. Slides were placed onto the heating stage and melted for 5 minutes at 195 °C, subsequently the samples underwent cooling at 20 °C/min to 140 °C where they were kept isothermally for crystallization to commence. Pictures were taken at set intervals (0; 5; 10; 20…100 minutes) in order to monitor the growth rate. The data was analyzed using Axiovision software.

3.3 References

1. Kirkegaard, P., Pedersen, N. and Eldrup, M. *PATFIT-88: a data-processing system for positron annihilation spectra on mainframe and personal computers*. (1989).

2. Botha, L. and Van Reenen, A. J. The effect of in-process ethylene incorporation on the evolution of particle morphology and molecular characteristics of commercial heterophasic ethylene propylene copolymers (HEPCs). *Eur. Polym. J.* **49,** 2202–2213 (2013).

Chapter 4:

4.1 Results and discussion of part II

4.1.1 Permeability testing

Permeability of the four selected samples (heterophasic ethylene-propylene copolymers) was determined [Table 4.1]. A general trend of increasing permeability could be observed with respect to the ethylene content of the copolymers. As the ethylene content increases so does the permeability. This is due to increasing ethylene sequences being incorporated and disrupting the crystallizing ability of the isotactic polypropylene sequences[1,2] and affecting the crystallization kinetics [Section 4.1.2]. Ethylene has a higher reactivity than propylene and will preferentially "homopolymerize" allowing few propylene insertions. This is potentially important at high ethylene concentrations. These copolymers with long ethylene sequences also crystallize and tend to pool[3] in specific areas which could also affect the permeability. Understanding the morphology and effect thereof on the increasing permeability needed to be investigated which means that the effect of ethylene incorporation on crystallinity would have to be probed. Crystallinity and fractional free volume (FFV) are closely related which therefore resulted in a closer examination of these properties.

Table 4.1: Permeability results.

Sample name	Ethylene Content (mol %)	Permeability $(\frac{\frac{kPa}{day}*cm}{cm^2*kPa})^2$
T_0	0	3.46×10^{-4}
T_30	2	5.61×10^{-4}
T_90	6.8	5.71×10^{-4}
T_150	9.3	7.35×10^{-4}

[2]Permeability experiments were conducted on an average of two times per sample with an error of less than 10%.

In the graph of permeability versus ethylene concentration [Figure 4.1], we notice that there are three distinct regions (S1, S2 and S3 corresponding to the samples containing 0 - 2, 2 - 6.8 and 6.8 - 9.3 % ethylene respectively). These three regions exhibit three different trends. As can be seen the permeability tends towards a plateau in the middle section (S2). Sample T_0 and T_30 do however show a larger error than the rest of the samples. This leads us to believe that small amounts of ethylene inclusion has a clear but inconsistent effect on the permeability, we therefore conducted a PALS experiment to investigate this phenomena.

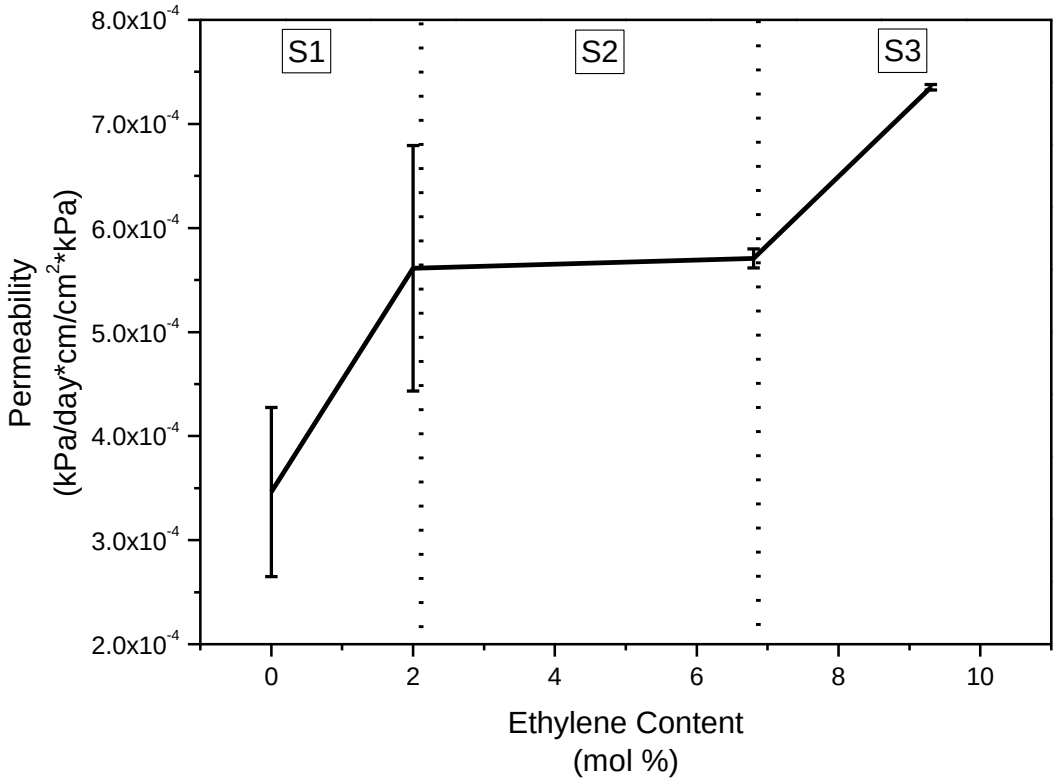

Figure 4.1: HEPC's permeability results

4.1.2 Positron annihilation lifetime spectroscopy (PALS)

According to free volume law, the increasing permeability obtained from the test results should be accompanied by an increasing fractional free volume (FFV)[4]. This is indeed the case as can be seen from Table 4.2. Figure 4.2 illustrates an overlay of sample permeability and FFV as a function of ethylene content. In S1 [Figure 4.1] we see a simultaneous increase in both

parameters, S2 exhibits a constant permeability with an increasing FFV, and in S3 the permeability increases greatly again with FFV tending to plateau. The reason for these trends might be explained through conducting multi-dimensional analysis (TREF, SEC-FTIR-HPer DSC, and High temperature 2D-LC) on the micro-structure of these complex polymers, which was what Botha et al. as well as Cheruthazhekatt et al.[5,6] had done previously. They noticed an effect that, as more ethylene is incorporated into the copolymer, shorter chains of PP and longer chains of PE with a higher crystallizing ability were formed. This, leads to small PP crystallites and larger PE crystallites being formed apart from the already existing PP crystalline structures formed during homopolymerization in the first reactor. Thus two events are occurring subsequently or simultaneously; the one event is ethylene inclusion into the porous PP homopolymer particles leading to some swelling of the particles with the other occurrence being the copolymer and ethylene homopolymer covering these particles and pooling around them. A large error in permeability around the lower ethylene inclusion range might be due to little or no effect of these two occurrences, and thereafter with higher ethylene inclusion these occurrences have a more uniform effect on the permeability.

These three areas denoted in Figure 4.2 below had to be investigated further to determine what the major influence on permeability is. Another property closely related to permeability is crystallinity, we therefore conducted a DSC experiment.

Table 4.2: PALS results.

Sample Name	Ethylene Content (mol %)	Permeability $\left(\frac{\frac{kPa}{day}*cm}{cm^2*kPa}\right)$	Fractional free volume (%)
T_0	0	3.46×10^{-4}	2.59
T_30	2	5.61×10^{-4}	2.73
T_90	6.8	5.71×10^{-4}	3.08
T_150	9.3	7.35×10^{-4}	3.15

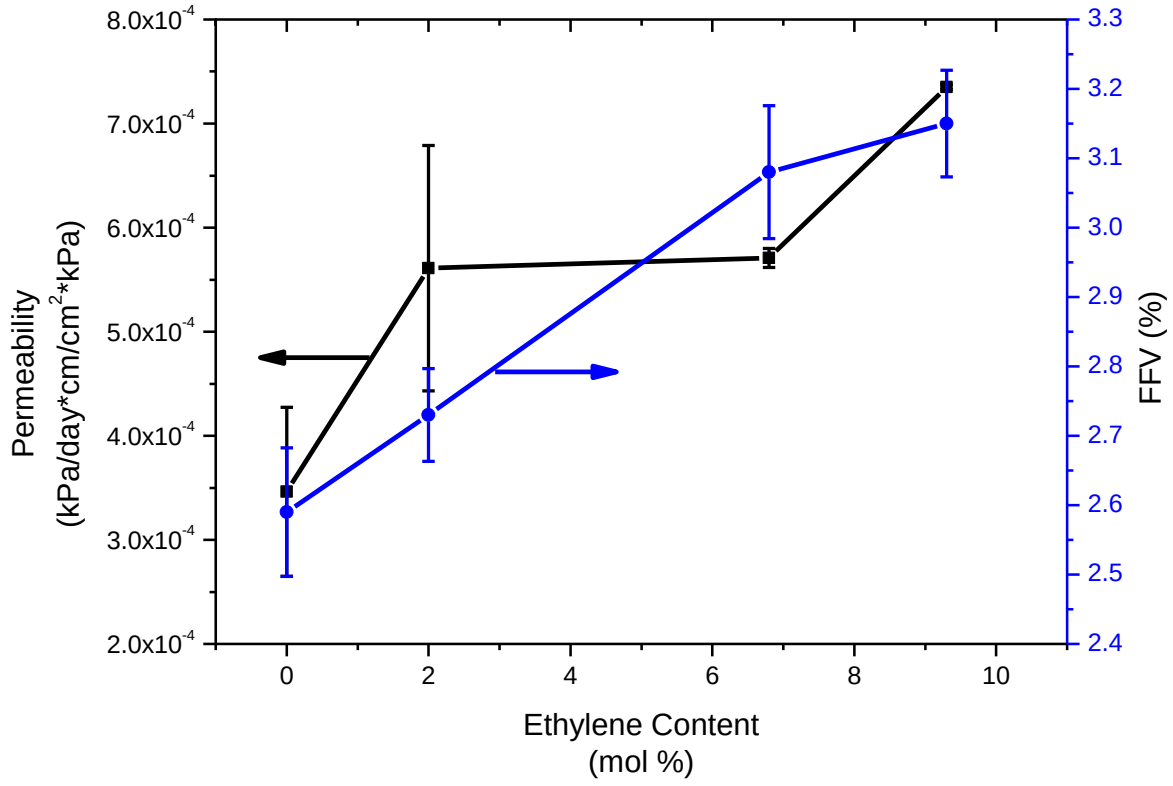

Figure 4.2: Permeability and FFV versus ethylene content.

4.1.3 Differential scanning calorimetry (DSC)

Crystallinity measurements were obtained for all four samples. Each sample was individually analyzed according to its ethylene content i.e. the reference heat of fusion used was corrected for the amount of ethylene in each sample. For sample T_0 (100 % isotactic polypropylene) 207 J/g was used as reference heat of fusion[7]. In order to correct for ethylene inclusion in the reference heats of HEPCs the following equation was introduced.

$$H_f^* = H_f^{iPP} \cdot \% C2 \qquad \textbf{Equation 4.1}$$

Equation 1 could then be substituted into crystallinity equation:

$$X_c^{PP} = \frac{H_f^{PP}}{H_f^{iPP}} \qquad \textbf{Equation 4.2}$$

$$X_c^{B} = \frac{H_f^{B}}{H_f^{*}} \qquad \textbf{Equation 4.3}$$

Where:

- H_f^* = Reference heat of fusion for blend.
- H_f^{iPP} = Reference heat of fusion for iPP.
- $\%C2$ = Percentage ethylene in blend.
- X_c^{PP} = Crystallinity of PP (Calculated from DSC).
- H_f^{PP} = Heat of fusion of PP.
- X_c^{B} = Crystallinity of blend.
- H_f^{B} = Heat of fusion of blend (Calculated from DSC).

Two sets of samples were analyzed. First the powder (nascent) form was analyzed and then a second set was analyzed in the form of a pressed film with added stabilizer (this was done to relate the crystallinities to the permeability specimens which were also pressed). As can be noted from Table 4.3, for the melt-pressed samples T_150 had a lower crystallinity than T_0, while the powder samples do not exhibit this trend. This can lead us to believe that the melt-pressing process had a big influence on the bulk crystallinity as well as the type of crystal formed in the samples (as opposed to the nascent polymer powders). It needs to be stressed that this observation is not merely due to the melting process of the nascent powders; during the DSC experiment the representative data is taken from the second heating cycle. This means that the powder samples are molten, cooled and re-melted. Melt-pressed samples differ from powder samples in that they are cooled more rapidly during the melt-pressing process, and this apparently results in crystalline structures that are different from the nascent powders. The fact that we can observe this trend in a DSC experiment during the second (heating) cycle indicates that the first heating cycle does not eliminate the thermal history completely, the type of crystals formed during pressing are thus recrystallized in the same environment and shape as was imparted on them by the applied pressure and heat in the melt press. It can therefore be concluded that the processed polymer is physically changed to a much greater extent than

expected and not through only analyzing the nascent polymer. Prediction of material properties needs to take processing parameters into consideration. It is clear that ethylene incorporation does initially decrease the crystallinity. Total crystallinity stays relatively constant as the amount of ethylene incorporation increases further. Nevertheless, this increase in ethylene incorporation causes the permeability and FFV to change markedly. All of this points to the need to investigate if and how the crystalline morphology is influenced through processing. To achieve this, X-ray diffraction studies were undertaken and discussed later.

Table 4.3: Summary of DSC results.

		Powder	Melt pressed
Name	Ethylene content (mol %)	Crystallinity (%)	Crystallinity (%)
T_0	0	37.5	42.5
T_30	2	35.9	36.1
T_90	6.8	39.0	36.8
T_150	9.3	37.6	37.0

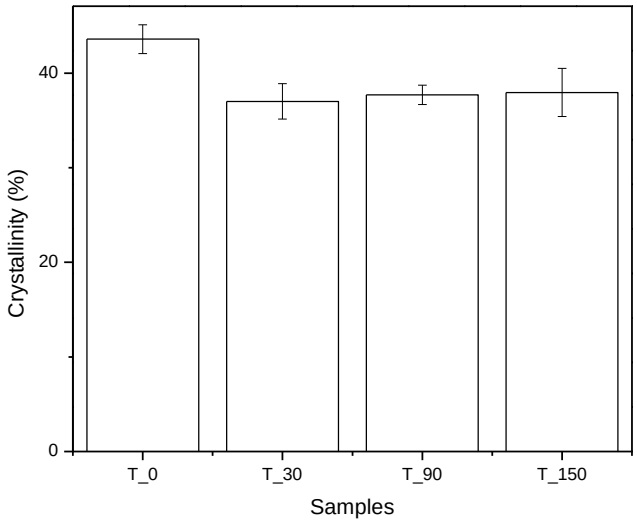

Figure 4.3: DSC results (melt-pressed samples).

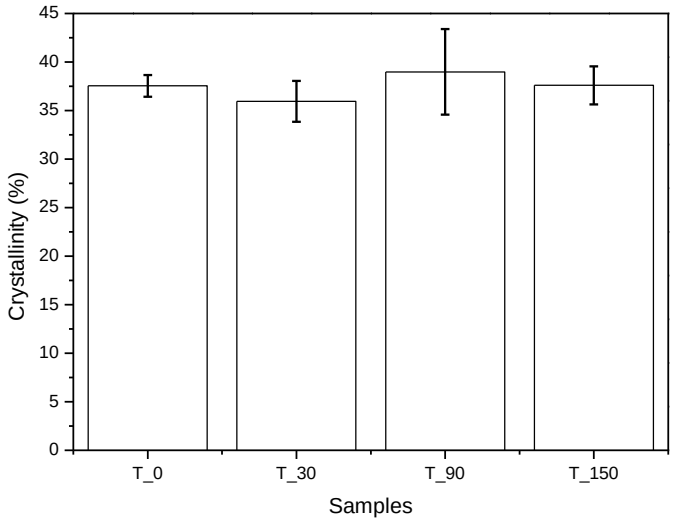

Figure 4.4: DSC results (powder samples).

SSA would therefore help to investigate the effect of ethylene incorporation on the crystalline structure [Figure 4.5]. In the PP melting region (170 – 180 °C)[8] two peaks could be observed with the lower temperature peak diminishing as ethylene content is increased. This observation would suggest that the higher fraction consists of highly isotactic PP and stays intact with increasing ethylene content; the slightly lower temperature melting peak is thus affected more

significantly by the ethylene inclusion. This is confirmed by deconvolution and integration of the peak areas which is illustrated in Figure 4.6. The result implies that the less isotactic material is not able to crystallize as ethylene is included and the material shift to an even lower crystallizing temperature or do not crystallize at all. This can be confirmed by noticing a slight exothermic peak around 120 °C for samples which might be indicating some polyethylene crystals forming [Appendix]. This polyethylene crystallinity was also observed by Botha et al.[5] who conducted solid state NMR experiments on these samples.

Visual investigation was conducted on the samples by means of polarized-light optical microscopy, to observe the effects of ethylene inclusion.

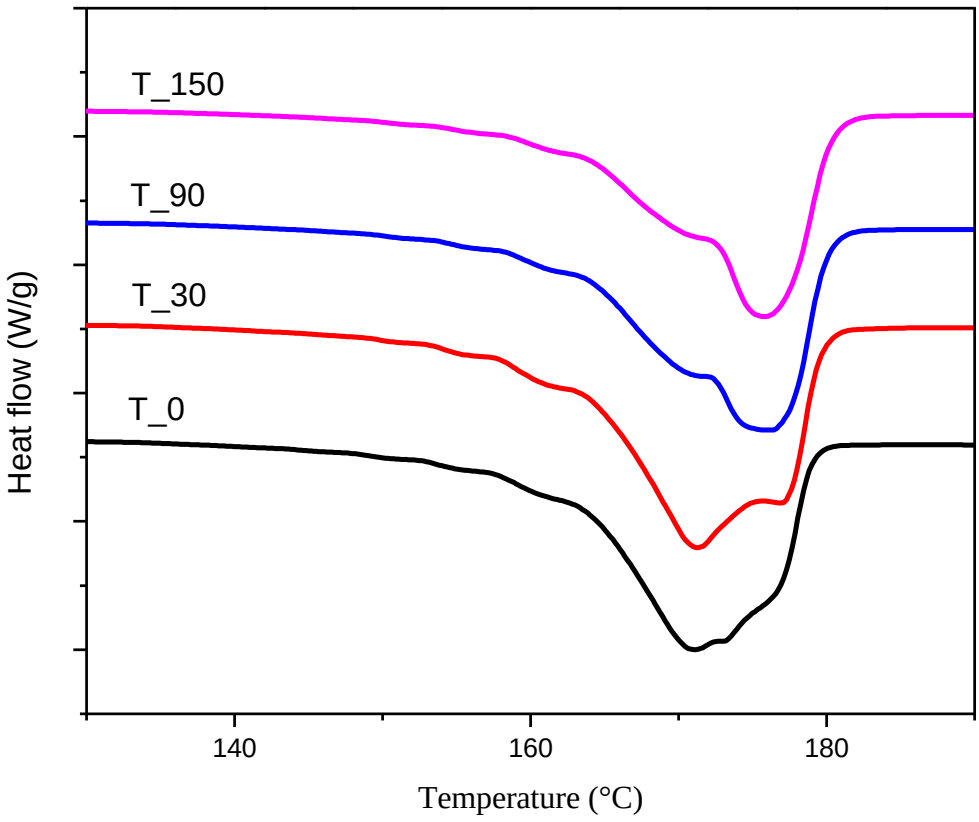

Figure 4.5: SSA thermograms (exothermic up).

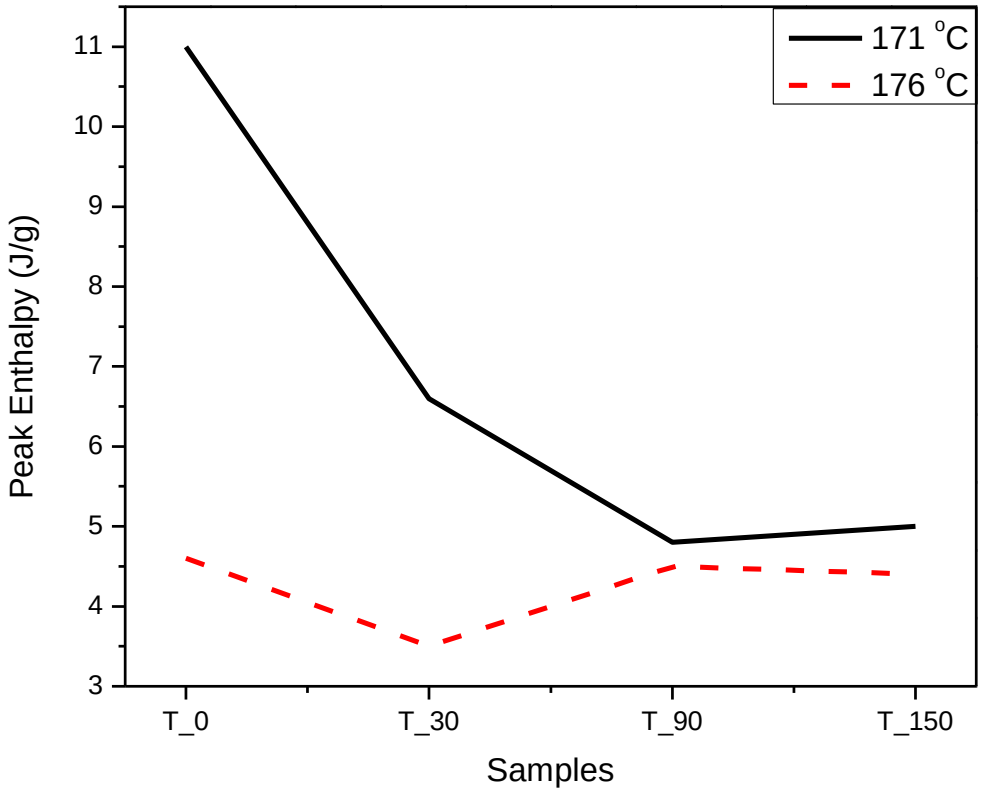

Figure 4.6: SSA melting peak enthalpy at 171 °C and 176 °C.

4.1.4 X-ray diffraction (XRD)

XRD patterns showed the presence of α and β crystalline forms for polypropylene diffraction peaks [Figure 4.7]. The most prominent change was observed in the β(300) peak which increased in intensity with an increase in ethylene content. In order to calculate the β-content the following Turner-Jones[9] equation was implemented:

$$K_{XRD} = \frac{A_\beta(300)+A_\beta(301)}{A_\beta(300)+A_\beta(301)+A_\alpha(110)+A_\alpha(040)+A_\alpha(130)A_\alpha(040)}$$ **Equation 4.4**

Where:

A = Area of peak

α = Alpha phase crystal

β = Beta allomorph

(###) = Crystal-face annotation (Figure 4.7)

Crystallinities were determined by deconvolution and integration of diffraction peaks [Figures 4.8 and 4.9].

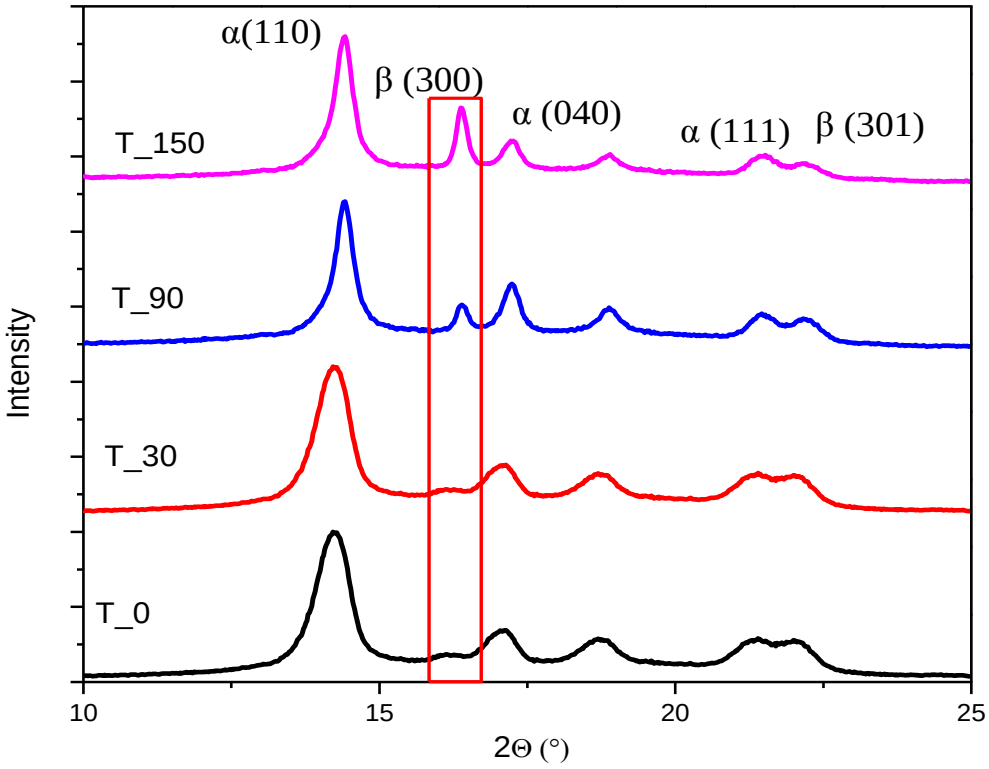

Figure 4.7: XRD data as well as peak annotation.

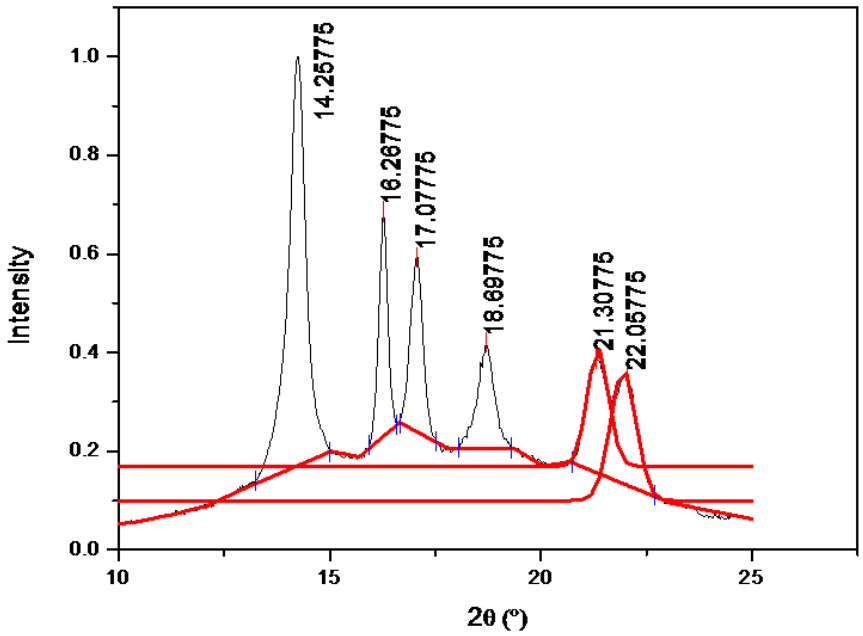

Figure 4.8: XRD spectrum with amorphous halo.

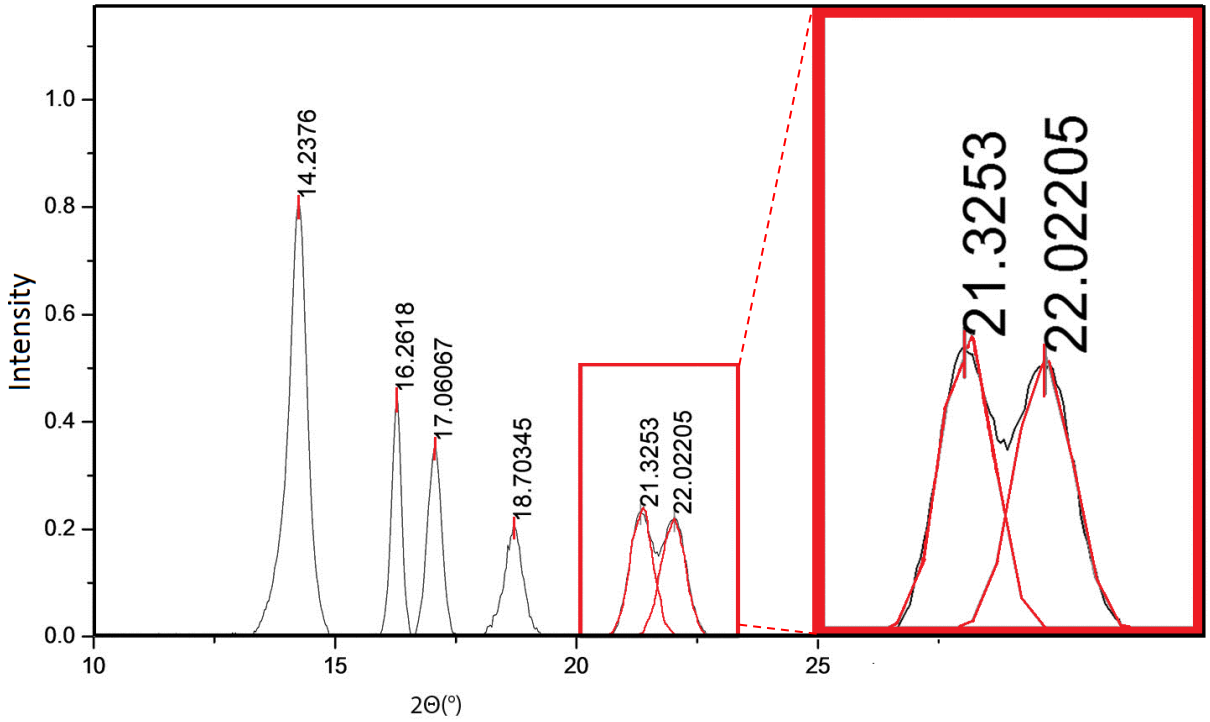

Figure 4.9: Deconvolution of XRD signals after amorphous halo removal.

A similar trend of decreasing crystallinity with ethylene inclusion was observed in the XRD results as in the DSC study for the melt-pressed samples [Table 4.4]. We need to take care when comparing XRD with DSC as these two techniques determine the degree of crystallinity utilizing different parameters. DSC calculates extent of crystallinity based on the heat of fusion and in XRD the diffraction pattern of polypropylene is used to determine the crystallinity. Both methods can, however, be used as an indication of general trends encountered in a material's crystallinity. Powder samples gave different results compared to melt-pressed samples and were also inconsistent as can be seen by comparing powder run 1 and 2. In the melt pressed samples, it could be observed that the amount of β-crystallinity (X_β) increases with the amount of added ethylene which might be the reason for increased permeability. Inconsistencies observed in the nascent samples compared to that of melt pressed samples must be due to the polymers being heterogeneously spread after sampling. After the melt pressing process the effect of ethylene inclusion seem to be homogenously spread throughout each sample.

Table 4.1: XRD crystallinities of Melt pressed and powder samples.

Melt Pressed				
Name	Ethylene Content (wt %)	X^3_T	X^4_α	X^5_β
T_0	0	45.99	87.04	12.96
T_30	2	44.72	83.31	16.69
T_90	6.8	34.21	81.04	18.96
T_150	9.3	32.41	79.41	20.59

Powder run 1[6]				
Name	Ethylene Content (wt %)	X_T	X_α	X_β
T_0	0	44.82	84.09	15.91
T_30	2	48.85	85.58	14.42
T_90	6.8	41.14	85.79	14.21
T_150	9.3	40.38	83.69	16.31

[3] Total crystallinity
[4]Alpha crystallinity
[5]Beta crystallinity
[6] Powder samples were melted in the DSC before they were placed in the XRD.

Powder run 2				
Name	Ethylene Content (wt %)	X_T	X_α	X_β
T_0	0	47.57	86.99	13.01
T_30	2	45.5	82.81	17.19

Investigation was done on the effect of isothermal treatment of the samples to observe the effect on X_β. In isothermal test 1 it was observed that keeping the sample just above its crystallization temperature (T_C = 125 °C) for 30 and 120 minutes decreased the alpha crystals (X_α) and increased X_β equivalently thus confirming the conversion of α crystals to the β form. This conversion, however, was only observed when the sample was subjected to a small amount of strain (as in the DSC pan constriction on the sample). If no strain is applied as in the case of using an isothermal oven crystallization technique (isothermal test 2), the opposite occurs and β-crystallinity decreases (Table 4.6). The effect on crystal structure was also more prominent in the sample with the highest ethylene content. Permeability tests were conducted on an isothermally treated sample of T_150 to see if β-crystallinity played a role in the permeability.

Table 4.4: Isothermal crystallization employing DSC.

		Isothermal test 1			
Name (Time)[7]	Isothermal time (min)	X_T	X_α	X_β	Conversion(α-β)
T_0	0	45.16	85.51	14.49	
T_0_30	30	46.74	82.71	17.29	2.80
T_150	0	40.35	83.85	16.15	
T_150_30	30	37.38	75.83	24.17	8.02
T_150_ 120	120	34.92	73.39	26.61	10.45

In this isothermal test the samples were kept above T_C in an oven. It can be seen that X_β decreased with time which contradicts our findings from the DSC experiment. External pressure

[7] Time kept isothermally

from the DSC pan thus induced β-crystallization whereas in the case of the oven experiment where no external pressure is exerted we find that the crystal structure could undergo some form of relaxation which reduces β-crystallization.

Table 4.5: Isothermal crystallization done in heated oven.

Isothermal test 2					
Name (Time)	Permeability $(\frac{\frac{kPa}{day}*cm}{cm^2*kPa})$	X^8_C	X_T	X_α	X_β
T_150_0	$7.78x\ 10^{-4}$	37.77	34.71	72.15	27.85
T_150_30	$7.64x\ 10^{-4}$	38.40	40.27	79.19	20.81
T_150_120	$6.17\ x\ 10^{-4}$	38.76	42.12	81.42	18.58

As it can be seen from the plot of β-crystallinity and permeability [Figure 4.10], X_β is related to the permeability to some extent. In samples T_0 to T_150 the permeability gradually increases with X_β. A remarkable trend was however observed when doing isothermal crystallization studies on sample T_150, and presented in Figure 4.11. X_β decreased with longer isothermal exposure times till the point where sample T_150_120 (isothermal test 2) exhibited comparable amount of X_β to that of sample T_90 (non-isothermal cooling) and quite remarkably the same permeability as well. These two samples have different ethylene contents, but by merely alternating their crystallization conditions their macroscopic properties can be similar.

This finding leads us to believe that there is a big effect on permeability through the crystallization kinetics and not only crystal structure. Crystallization kinetics were thus investigated by making use of a polarizing optical microscope technique [Chapter 3].

[8]DSC determination of crystallinity

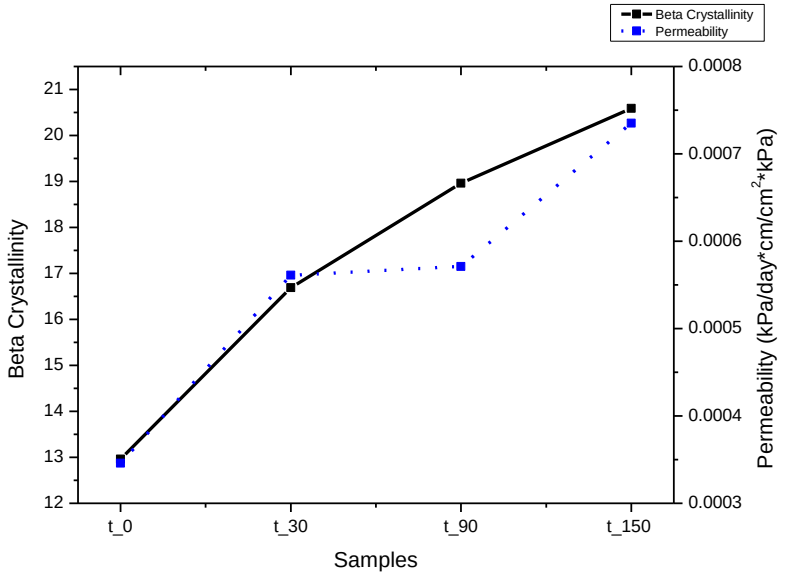

Figure 4.10: Non-isothermal cooling experiment (β-crystallinity and permeability versus ethylene inclusion).

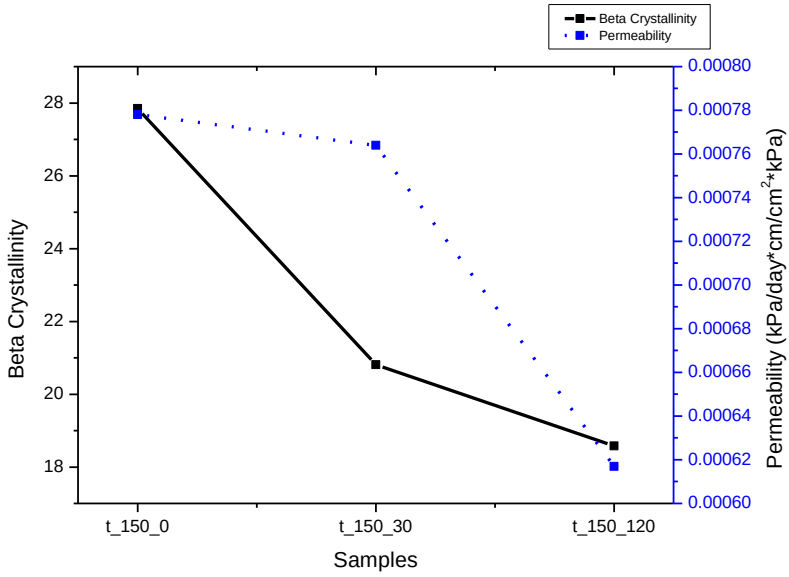

Figure 4.11: Isothermal crystallization experiment (β-crystallinity and permeability versus ethylene inclusion).

4.1.5 Polarized-light optical microscopy (POM)

Radial growth rate of each sample was successfully determined using the following equation:

$$G = \frac{dR}{dt} \qquad \textbf{Equation 5}$$

Where:

- R = radius of spherulite
- t = time

Ethylene inclusion did not seem to have any great effect on crystal size nor the growth rate [Figure 4.12]. As ethylene is increased the crystal size and growth rate does seem to increase slightly as in the case of sample T_30. For sample T_90 it stays in the same range, then again for sample T_150 there is a drop back to the same crystal size and growth rate suggesting that there is no significant effect of ethylene inclusion on crystal growth rate. On the other hand, a visual inspection was conducted and it could be observed that the ethylene inclusion had an effect on crystal morphology. Birefringence was distorted as ethylene content increased [Figure 4.13]. This was caused by the fact that β-crystallinity exhibited negative birefringence[10] (indicated by arrows). Slow cooling allowed for larger more uniform crystals to form and when fast (non-isothermal) cooling [Figure 4.14] was experienced it results in more nucleation sites being present resulting in more crystals and therefore more crystal boundary interfaces which could allow for permeation of a gas far better that a single large crystal which only allows permeability through its β-crystal sections.

This phenomenon was also observed by Botha et al.[5] after conducting a solid state NMR experiment wherein she explained that methylene groups experience something called the gauche effect. These groups are in different chemical environments due to added ethylene crystallizing around them. This might explain the section S2 in Figure 4.1 wherein FFV increases due to imperfect packing. In section S3 this effect might be saturated and ethylene causes problems of a different nature.

Table 4.6: Radial growth rates as a function of ethylene inclusion.

Sample name	G (µm/min)
T_0	1.08
T_30	1.43
T_90	1.46
T_150	1.21

However if faster cooling rates (> 20 C/min) are introduced, more nucleation sites are formed at the same time leading to more crystals forming which results in more crystal surface boundaries i.e. more rigid amorphous phase (RAF) which also consists of more free volume than a single solid crystal.

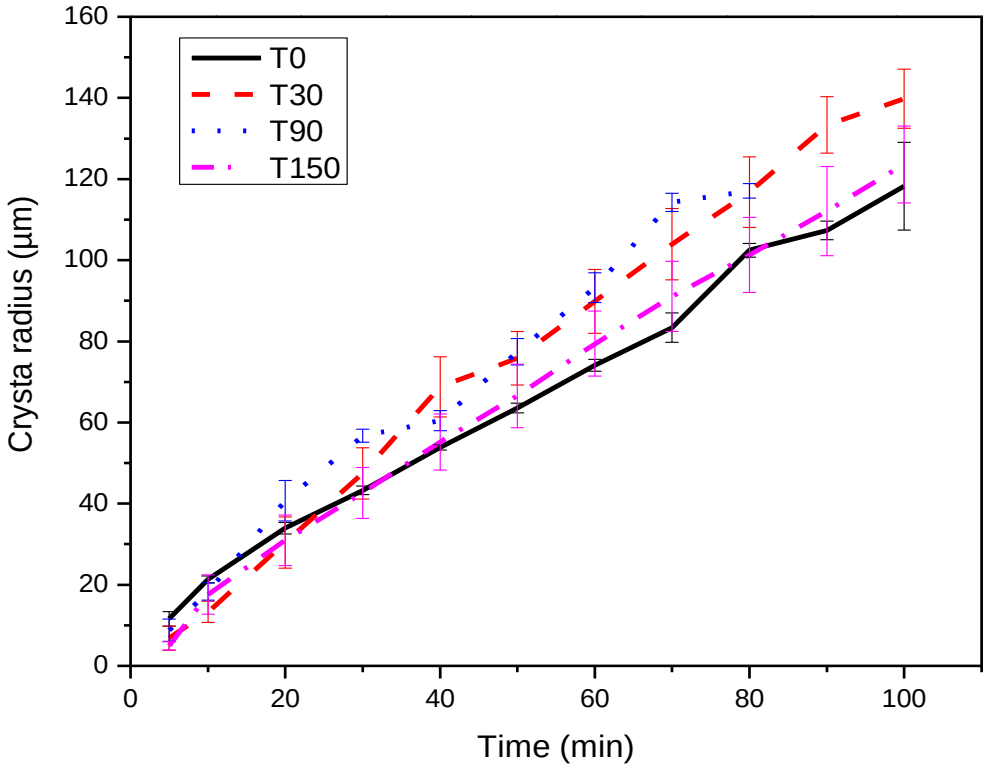

Figure 4.12: Radial growth rate of samples.

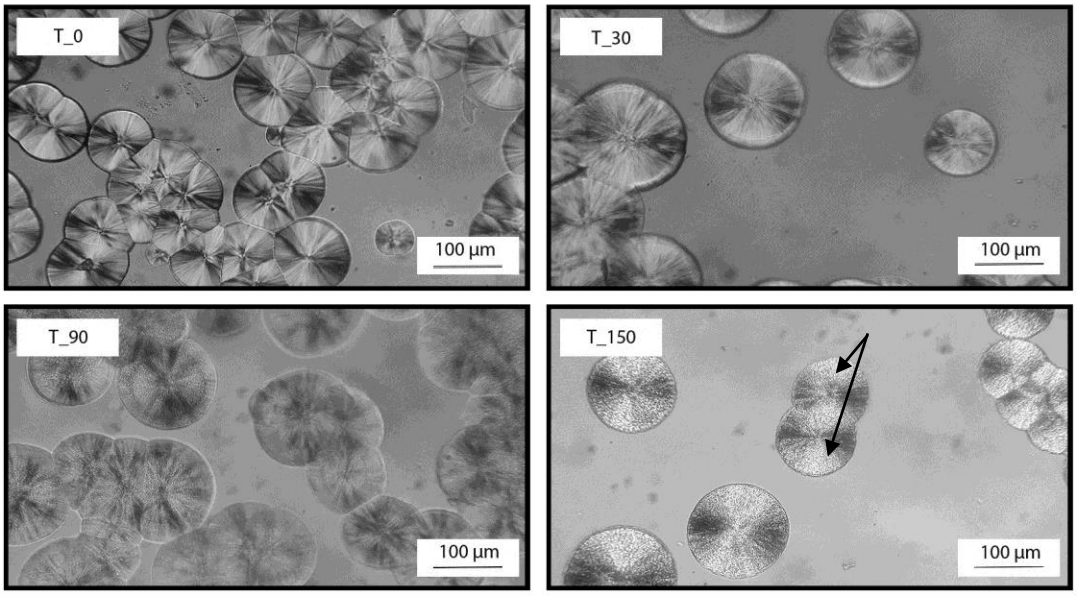

Figure 4.13: Slow cooled optical micrographs of HEPCs after 50 minutes at 140 °C (Scale bar = 50 µm).

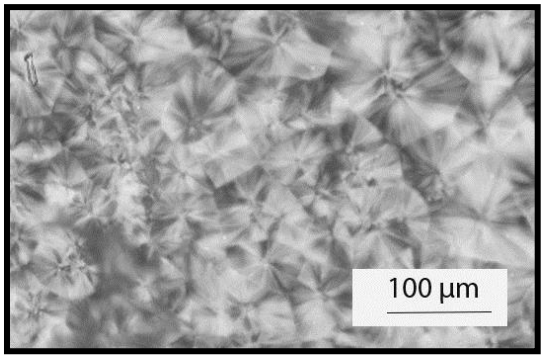

Figure 4.14: Non-isothermally fast cooled optical micrograph of HEPCs (Sample T_0 growth saturation = 2 minutes.)

4.2 Part two: Conclusion

In part two, a definite relationship between gas permeability and ethylene inclusion was shown. Despite the general increasing permeability trend seen, the graph showed three distinct regions of interest. In the first region with only small amounts of ethylene inclusion (2 %) a distinct

increase in permeability was observed. Thereafter a plateau was observed as no great increase in permeability occurred until about 6.8 % where once again a sudden increase in permeability occurred. Further investigation into the cause of permeability on a morphological level was also conducted.

Fractional free volume, crystallinity and type of crystallinity all have been established to have a direct relationship towards the permeability. FFV results showed a good relationship towards permeability as was expected although no plateau was observed in region 2 as in the trend seen from the permeability results. The reason for this was attributed towards the permeability measurements having a large error reading with small amounts of ethylene inclusion meaning the ethylene was included inconsistently at such low concentrations. DSC crystallinity measurements did show a decreasing polypropylene crystallinity with small amounts of ethylene inclusion, but extra ethylene did not decrease the total crystallinity further. We could therefore conclude that here are two distinct events taking place related to the crystallinity. In the first event (with only small amounts of ethylene introduction) the ethylene interferes with the PP spherulites which decreases the crystallinity, when the porous PP spherulites are filled with PE and with more ethylene inclusion the PE deposits onto the spherulites where it does not interfere with the crystallinity but still affects the permeability and FFV. This statement could be substantiated by the SSA experiment which showed that with more ethylene inclusion the more imperfect PP (lower melting point) crystals being diminished. Interestingly XRD coupled with isothermal experiments showed an excellent relationship between β-crystallinity and permeability and an even closer relationship with FFV. The crystal imperfections could also visually be observed through polarized-light optical microscopy wherein negative birefringence which is indicative of β-crystallinity increased with ethylene inclusion. All of these factors have to be considered as a whole and not individually when a prediction on a material's permeability is to be made. Lastly the effect of cooling rate also had a big influence on permeability and crystal form, where slower cooling allows for better crystal formation hence less crystal imperfections and therefore better permeability. The effect of ethylene inclusion on the mechanical properties are well known[11;12], and now we have drawn a relationship to permeability as well.

4.3 References

1. van der Meer, D. W., Varga, J. and Vancso, G. J. The influence of chain defects on the crystallisation behaviour of isotactic polypropylene. *Express Polym. Lett.* **9,** 233–254 (2015).

2. Harding, G. The fractionation and characterisation of propylene-ethylene random copolymers. *MSc Thesis Stellenbosch Univ.* (2005).

3. Botha, L. and Van Reenen, A. J. The effect of in-process ethylene incorporation on the evolution of particle morphology and molecular characteristics of commercial heterophasic ethylene propylene copolymers (HEPCs). *Eur. Polym. J.* **49,** 2202–2213 (2013).

4. Park, J. Y. and Paul, D. R. Correlation and prediction of gas permeability in glassy polymer membrane materials via a modified free volume based group contribution method. *J. Memb. Sci.* **125,** 23–39 (1997).

5. Botha, L., Sinha, P., Joubert, S., Duveskog, H. and Van Reenen, A. J. Solution and solid-state NMR characterization of heterophasic propylene-ethylene copolymers (HEPC) with increasing ethylene content. *Eur. Polym. J.* **59,** 94–104 (2014).

6. Cheruthazhekatt, S., Pijpers, T. F. J., Harding, G. W., Mathot, V. B. F. and Pasch, H. Multidimensional analysis of the complex composition of impact polypropylene copolymers: Combination of TREF, SEC-FTIR-HPer DSC, and high temperature 2D-LC. *Macromolecules* **45,** 2025–2034 (2012).

7. Wang, S., Zhang, J., Chen, S. and Zhu, H. Crystal structure and melting behavior of homo-polypropylene and heterophasic ethylene–propylene copolymer after long time heat treatment. *J. Cryst. Growth* **355,** 151–158 (2012).

8. Maier, C. and Calafut, T. *Polypropylene : the definitive user's guide and databook*. (Plastics Design Library, 1998).

9. Jones, A. T., Aizlewood, J. M. and Beckett, D. R. Crystalline forms of isotactic polypropylene. *Die Makromol. Chemie* **75,** 134 (1964).

10. Iroshi Awaya, H. Morphology of different types of isotactic polypropylene spherulites crystallized from melt. *Polymer (Guildf).* **29,** 591–596 (1988).

11. Liang, J.Z. and Li, R. K. Y. Rubber toughening in polypropylene: A review. *J. Appl. Polym. Sci.* **77,** 409–417 (2000).

12. Jose, S., Aprem, A. S., Francis, B., Chandy, M. C., Werner, P., Alstaedt, V. and Thomas, S. Phase morphology , crystallisation behaviour and mechanical properties of isotactic polypropylene / high density polyethylene blends. *Eur. Polym. J.* **40,** 2105–2115 (2004).

Part III: Effects of chemical composition on the properties of HDPE/LDPE blended films.

Chapter 5:

5.1 Introduction

The third and final part of this study was done to further illustrate the findings obtained in part two. A polymer blend was investigated and an explanation of permeability behavior was attempted by means of a morphological study. A commonly used and suitable polymer blend wherein information on the permeability behavior is of economic value was chosen. This sample set is related to part one in the sense that it is also an incompatible, blend. The experiments were conducted on a series of high density polyethylene (HDPE) blended with varying low-density polyethylene (LDPE) content [Table 5.1].

5.2 Background: HDPE/LDPE blends

Two of the most used polyolefins globally are PE and PP with PE being the most popular. In 2015 the global consumption was 150 million tonnes with an expected growth of up to 5 % per annum[1]. The reason for their popularity is because of their beneficial mechanical properties, prolonged durability, low costs, easy manufacturing capability, and good chemical resistance[2,3]. The desire for blending of HDPE and LDPE is obvious because they exhibit very different yet favourable qualities wherein a combination thereof is highly beneficial to the industrial sector. In South Africa plastics are currently used in multiple applications with food packaging (53 % per annum)[4] being the most utilized.

Various research groups have studied the morphology and rheology of HDPE/LDPE blends, but little has been reported on the study of permeability properties[5]. Despite its importance research on the gas permeability behaviour of these blends of pure polyolefins without addition of expensive inner layers such as EVOH or polyamide (PA) has not been a key point of concern in the industry, which would be highly beneficial to especially the food packaging sector.

5.3 Sample preparation

Samples were prepared by solution blending the respective ratios (HDPE: LDPE; 15 g total weight) with a stabilizer mixture (50 % Irganox 1010 and 50 % Irgafos 165; 2 wt %). This was done under reflux in a round bottom flask (250 mL) dissolved using xylene (200 mL; 135 ^{0}C). The samples were then dried and melt-pressed into thin films (200 µm), which were used for testing (see Chapter 3.1.3). All test methods were conducted in the same manner as in part two (see Chapter 3.2).

5.4 Results and discussion

5.4.1 Permeability

Permeability results [Figure 5.1] are quite surprising as we expected an increase in permeability accompanying the increase in the more amorphous LDPE content. Interestingly the opposite effect was in fact observed as the permeability was decreased with addition of 10 wt % LDPE. After 20 wt % LDPE was added the permeability was decreased even further. Knowing that the permeability of pure LDPE is greater than that of pure HDPE some inflection point should be noticeable when increasing the LDPE content[8]. This was indeed the case as a deflection point was observed between 20 and 30 wt % LDPE thereafter the permeability increased linearly until it reached the highest point of permeability which was that of pure LDPE. The reason for this initial decrease in permeability is still unknown and should be further investigated. When 50 wt % LDPE was added the permeability surpassed that of pure HDPE. Permeability results are given in Table 5.1.

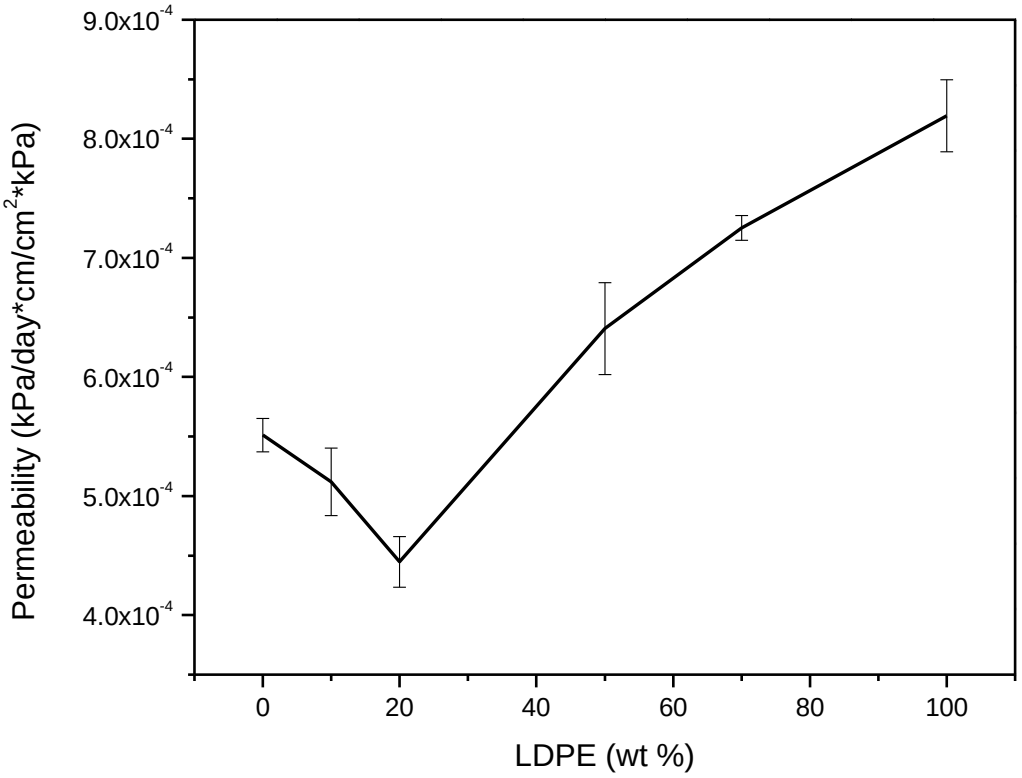

Figure 5.1: Permeability results of HDPE/LDPE blends.

Table 5.1: Blend compositions and permeability results.

Name	LDPE content (wt %)	Permeability ($\frac{\Delta t \cdot A \cdot \Delta p}{\Delta m_{gas} \cdot l}$)[9]
HDPE_0	0	$5.61\ x\ 10^{-4}$
HDPE_10	10	$5.31\ x\ 10^{-4}$
HDPE_20	20	$4.60\ x\ 10^{-4}$
HDPE_50	50	$6.68\ x\ 10^{-4}$
HDPE_70	70	$7.25\ x\ 10^{-4}$
LDPE	100	$8.19\ x\ 10^{-4}$

[9] Permeability experiments were conducted on an average of three times per sample.

5.4.2 Positron annihilation lifetime spectroscopy (PALS)

PALS data obtained correlated well with the permeability data found in part two of this study [Figure 5.2]. Results are summarized in Table 5.2.

Table 5.2: FFV results of HDPE/LDPE blends.

Name	LDPE content (wt %)	$Permeability\ (\frac{cm^3 \cdot mm}{m^2 \cdot day \cdot atm})$	Fractional free volume (%)
HDPE_0	0	$5.61\ x\ 10^{-4}$	3.84
HDPE_10	10	$5.31\ x\ 10^{-4}$	3.51
HDPE_20	20	$4.60\ x\ 10^{-4}$	3.36
HDPE_50	50	$6.68\ x\ 10^{-4}$	3.82
HDPE_70	70	$7.25\ x\ 10^{-4}$	3.78
LDPE	100	$8.19\ x\ 10^{-4}$	4.81

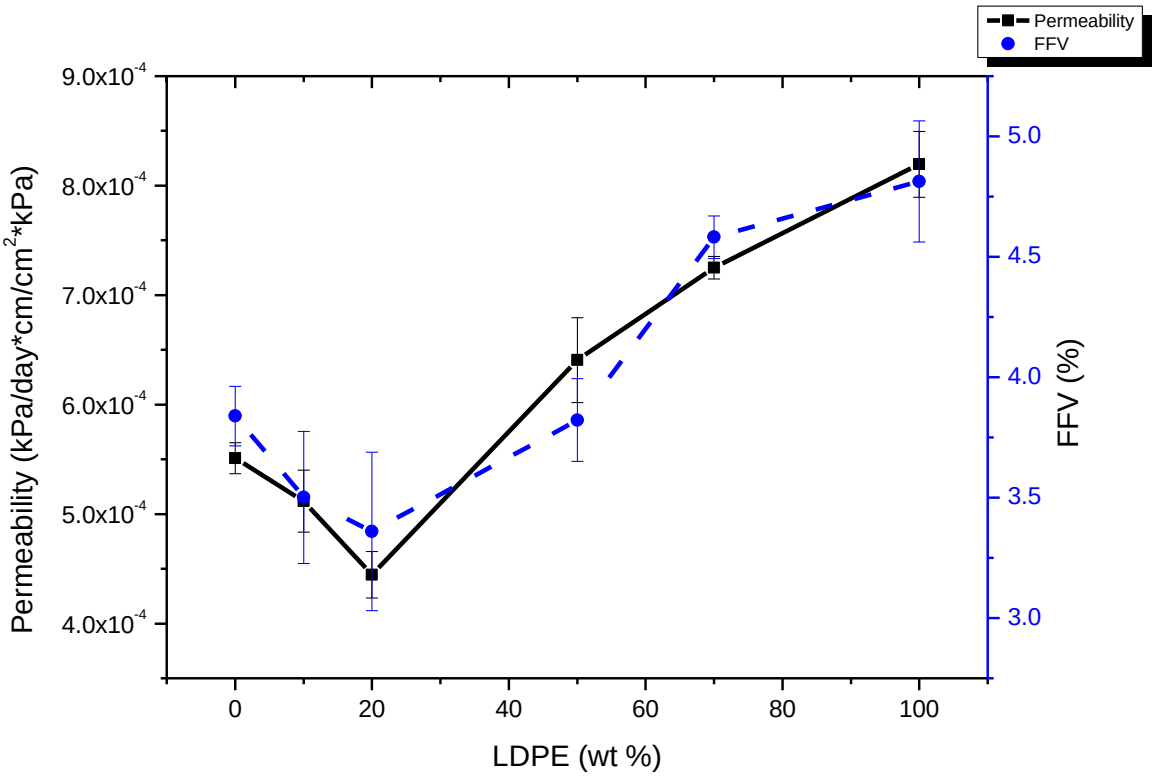

Figure 5.2: Permeability and FFV versus ethylene content.

Positron lifetime spectra were collected for each sample and evaluated with PATFIT software. Lifetime and intensity values were extracted from the spectra with a model function consisting of a sum of decaying exponentials convoluted with the resolution function of the lifetime spectrometer plus a constant background. The best fit was found to be from the fourth lifetime (τ_4) said to be associated with larger free volume holes due to blend incompatibility and less gas selectivity[6].

In another study done by Gomaa et al.[7] they also encountered a deviation in permeability from the linear increase with additive composition one would intuitively expect for blends, they concluded that this phenomena could be accounted for by interfacial boundaries having a greater effect than interspherulitic FFV. In their experiment they used nitrile butadiene rubber (NBR) blended with LDPE.

5.4.3 Differential scanning calorimetry (DSC)

Crystallinity studies did not prove to be very helpful in describing the permeability behavior. As can be seen from Figure 5.3 there was a clear decrease in total crystallinity up until 20 wt% LDPE where we expected an increase. The permeability then increases again and with it we observed a decrease in crystallinity, this decrease was expected to continue until pure LDPE, but instead we observe an increase for LDPE crystallinity which once again did not agree with the permeability data.

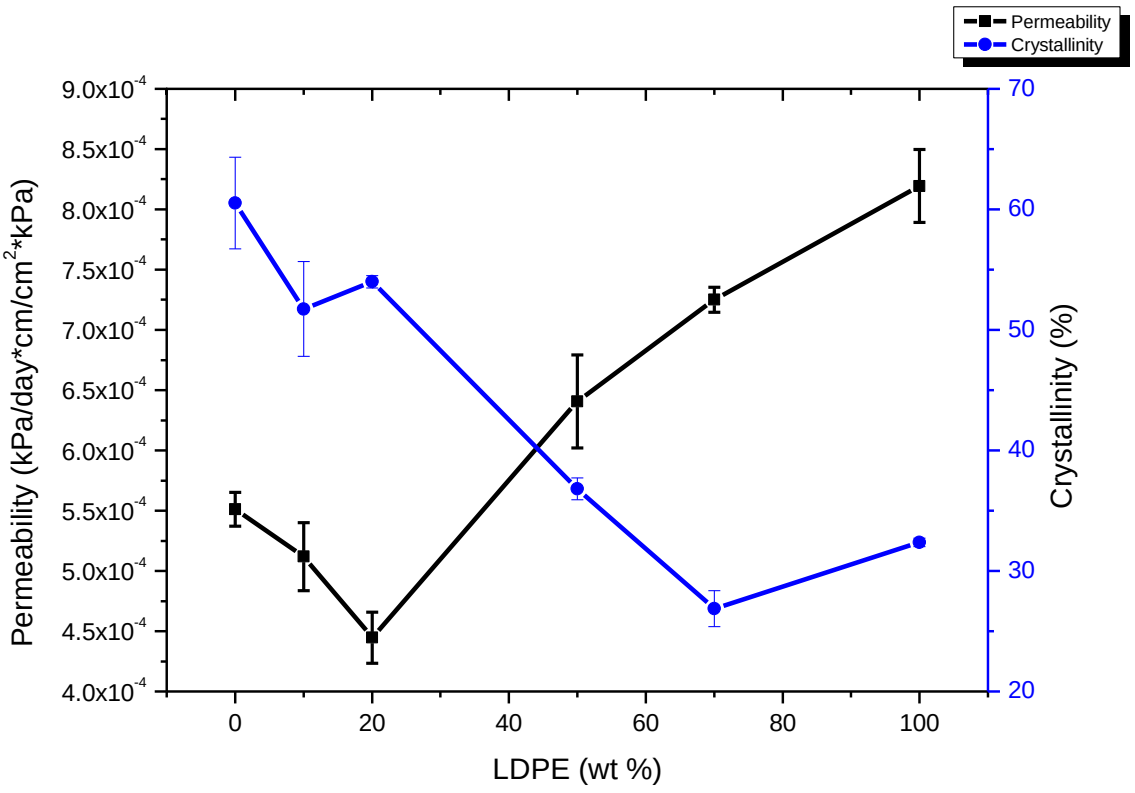

Figure 5.3: Permeability and DSC crystallinity versus LDPE (wt %)

DSC results did however prove that the blends were prepared correctly, as seen by incremental decrease in endothermic melting peaks around 130 °C as well as an increase in endothermic melting peak of LDPE around 110 °C [Figure 5.4]. Some idea of crystallization behavior is obtained, however when looking at the cooling cycle. One unusual occurrence is observed at the 90:10 blend where recrystallization takes place faster than for the pure HDPE.

Table 5.3: DSC crystallinity results summary for HDPE/LDPE blends.

Name	LDPE Content (wt %)	Crystallinity (%)		
		HDPE (120 -140 °C)	LDPE (100-115 °C)	Total
HDPE_0	0	60.52	0	60.52
HDPE_10	10	51.73	0	51.73
HDPE_20	20	54.00	0	54.00
HDPE_50	50	28.79	8.03	36.82
HDPE_70	70	15.85	11.02	26.87
LDPE	100	0	32.37	32.37

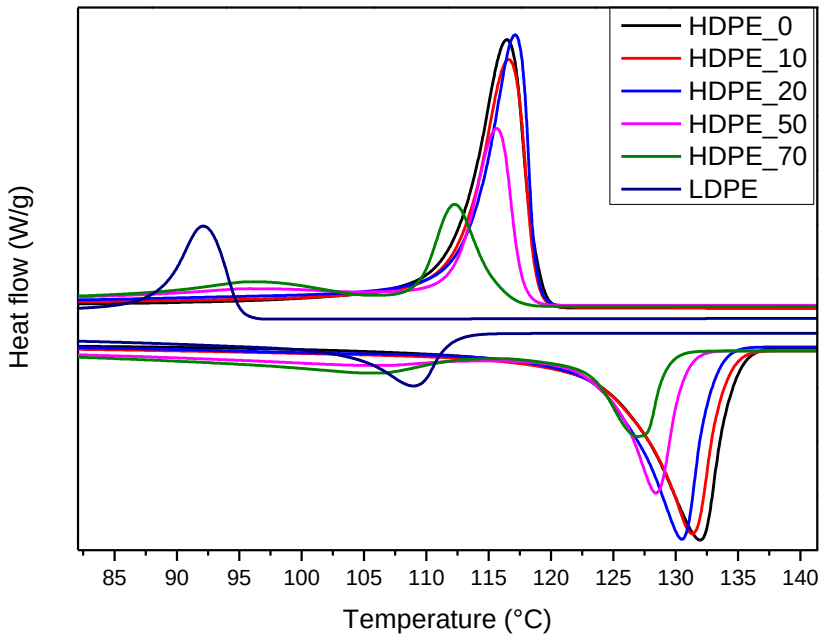

Figure 5.4: DSC data showing compositional drift.

5.4.4 X-ray diffraction (XRD)

From the permeability data [Table 5.4] an increase in crystallinity was expected to accompany the decrease in permeability up until 20 wt % LDPE, this was however not the case as a clear decrease in the crystallinity was observed. After 50 wt % LDPE inclusion, the crystallinity dropped again with the permeability increasing. These were contradicting results and were therefore not considered as a true reflection of the effect of crystallinity on permeability.

Table 5.4: XRD crystallinity results of HDPE/LDPE blends.

Name	Ethylene Content (wt %)	Crystallinity (%)
HDPE_0	0	50.12
HDPE_10	10	44.95
HDPE_20	20	41.57
HDPE_50	50	49.23
HDPE_70	70	31.77
LDPE	100	30.00

5.4.5 Polarized-light optical microscopy (POM)

POM was not effective in determining crystal growth rate as for the HEPCs in part two. The crystals were too small and when mounted on the heating stage the magnification could also not be increased. A different technique such as SEM which allows a higher resolution to be used should be implemented. It was however not done because the FFV data was deemed to provide sufficient explanation for permeability results observed. An example of the POM photographs can be seen in Figure 5. below.

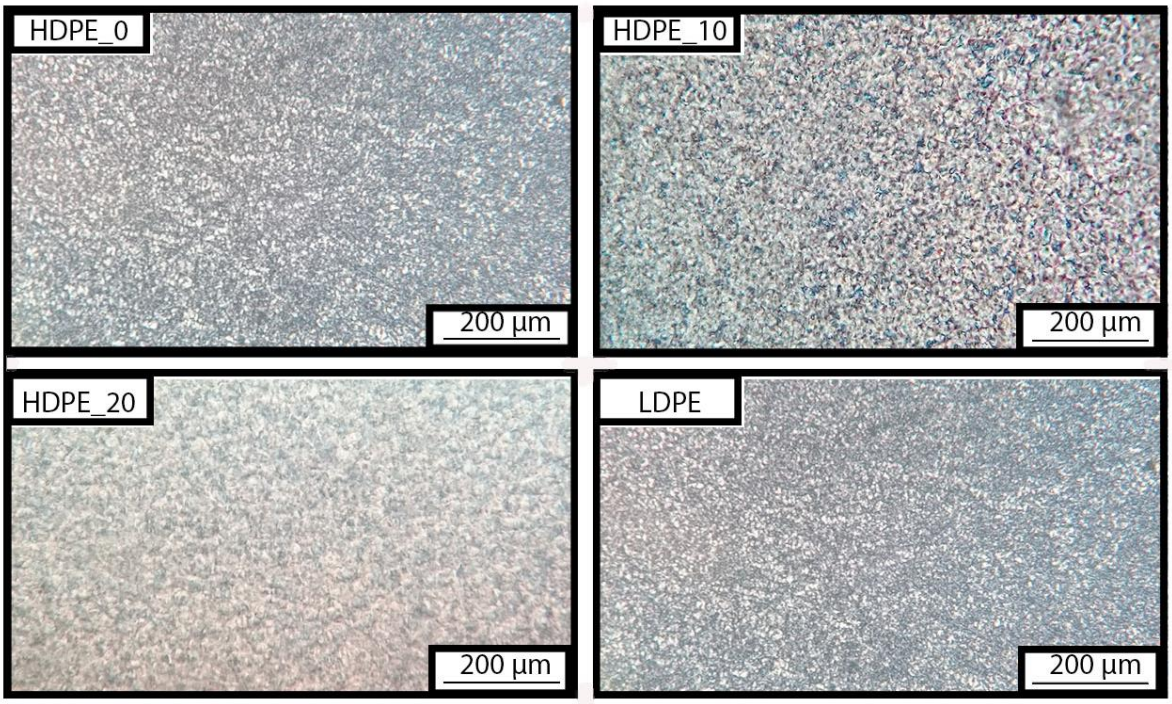

Figure 5.5: POM images of the pure samples and two of the blends.

5.5 Part III: Conclusion

Part three was successful in that a range of HDPE:LDPE blended films could be prepared and tested for permeability. Permeability results varied with composition and not as it was suspected to vary. An unexpected result was encountered when blending up to 20 wt% of more permeable LDPE to a HDPE matrix, the combination resulted in a less permeable film than pure HDPE. Results from a PALS experiment however confirmed this trend and substantiated the findings obtained in the permeability experiment. Crystallinity studies did not result in any useful information as it did not follow any trends which could be related to the permeability experiment, a similar problem to that encountered in part two. Percentage crystallinity of a film was therefore not a good means of predicting permeability. Fractional free volume on the other hand is much more accurate in predicting permeability in films, especially when the effects of additives play a determining role in a macro property.

5.6 References

1. Galiè, F. Global Market Trends and Investments in Polyethylene and Polypropylene. *Icis* 1–3 (2016).

2. Fu, Q., Men, Y. and Strobl, G. Understanding of the tensile deformation in HDPE/LDPE blends based on their crystal structure and phase morphology. *Polymer (Guildf).* **44,** 1927–1933 (2003).

3. Munaro, M. and Akcelrud, L. Correlations between composition and crystallinity of LDPE/HDPE blends. *J Polym Res.* **15**:83-88 (2008).

4. Lange, J. and Yves, W. Recent innovations in barrier technologies for plastic packaging - a review. *Packag. Technol. Sci.* **16,** 149–158 (2003).

5. Burns, D. E. and Ii, S. V. P. Technical Note on Cold Weather Installation of HDPE. *Geotextiles and Geomembranes* **9,** 457–459 (1990).

6. Shantarovich, V. P., Kevdina, I. B., Yampolskii, Y. P. and Yu Alentiev, A. Positron Annihilation Lifetime Study of High and Low Free Volume Glassy Polymers: Effects of Free Volume Sizes on the Permeability and Permselectivity. *Macromolecules **33***, 7453-7466 (2000).

7. Gomaa, E., Mostafa, N., Mohsen, M. and Mohammed, M. Correlation Between Free-Volume Parameters and Physical Properties of Polyethylene-Nitrile Rubber Blend. *Journal of Materials Engineering and Performance* **13**, 583-587 (2004).

8. Massey, L. K. *Permeability Properties of Plastics and Elastomers*. (Plastics Design Library, New York, (2003).

Chapter 6

6.1 Conclusion

In part one a preliminary study was done to develop a single layer dunnage bag formulation. Puncture resistance, permeability and yield strength were identified as the main properties of concern and an envelope was developed to evaluate these properties of films that are currently available. It was found that there was a distinct relationship between favourable and unfavourable properties, for example such as low permeability is generally accompanied by a high rigidity (EVOH27 for example) and high permeability is generally associated with a low rigidity as in the case of CMR348. This led to an attempt to create multilayer films using EVOH27 and CMR348 samples to achieve a combination of their properties. These samples were incompatible and required the use of a compatibilizer to create the films. This lead to, the expected physical properties but a decrease in permeability from the expected trend. It was therefore concluded that the effect of processing conditions when dealing with polymer blends could be a determining factor and thus a restrictive one within the scope of this study.

Heterophasic ethylene-propylene copolymers (HEPCs) were selected for further study as they comprised of favourable mechanical properties and the effect of ethylene inclusion seemed to greatly affect a film's permeability. This led to part two where permeability was successfully measured for an entire range of HEPCs and it was found that as the ethylene content increased the permeability increased accordingly, except for region S2 [Figure 6.1] where a plateau in the trend was encountered. This was ascribed to the large error reading for samples with small amounts of ethylene content as ethylene was included inconsistently at such low concentrations. An attempt was made to explain this observation through studying the change in morphology as ethylene content was increased. A positron annihilation lifetime spectroscopy experiment was carried out to observe the change in fractional free volume. These results correlated strongly with the permeability results and it could be concluded that the determination of the fractional free volume was the best method for predicting a polymeric film's permeability. Crystallinity experiments conducted through differential scanning calorimetry were not as conclusive. The

decrease in permeability could for the large part not be explained purely in terms of percentage crystallinity as the overall crystallinity remained relatively constant between 2 and 9.3 wt% ethylene inclusion. This observation was confirmed by SSA experiments which showed that ethylene inclusion only affects the lower temperature melting peak indicating an interference in the less perfect PP crystals. We could therefore conclude that there are two distinct events taking place related to the crystallinity. In the first event (with only small amounts of ethylene introduction) the ethylene interferes with the PP spherulites which decreases the crystallinity, when the porous PP spherulites are filled with PE or copolymer and with more ethylene inclusion the PE or copolymer deposits onto the spherulites where it does not interfere with the crystallinity but still affects the permeability and FFV.

X-ray diffraction showed that the β-crystal form of PP was induced by ethylene inclusion and correlated strongly with permeability. Where an increase in ethylene caused an increased β-crystallinity resulting in a higher permeability. This was also confirmed by conducting isothermal experiments coupled with XRD. Isothermal relaxation reduces β-crystals to the α-crystal form therefore simultaneously decreasing the permeability. Using polarized-light optical microscopy it was made possible to observe negative birefringence within the samples. Negative birefringence is indicative of β-crystals and was visually observable via isothermal crystallization. Herein we could also observe that fast cooling produced a greater amount of imperfect crystals which also led to a greater permeability.

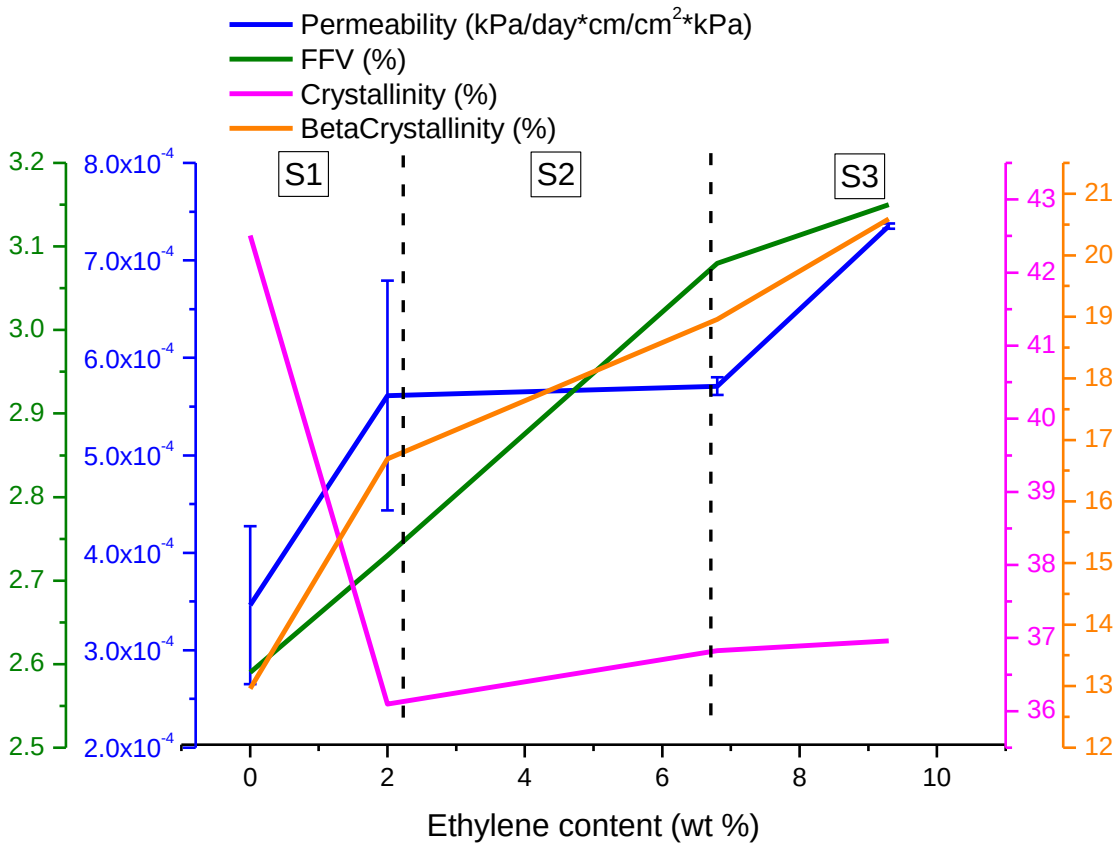

Figure 6.1: Combined graph of all the results in part two (HEPCs).

In part three where HDPE was solution blended with differing amounts of LDPE an interesting observation was made, in that when small amounts of more permeable LDPE was added (below 20 %) there was a counterintuitive decrease in the permeability. This was confirmed via a PALS experiment where the trend of FFV and permeability was clearly demonstrated. The reason for this is still not clear but could be due to the interfacial tension between immiscible blends creating bigger FFV holes at low concentrations. Crystallinity studies did not result in any useful information as it did not follow any trends which could be related to the permeability experiment, similar to the problems encountered in part two of the study. DSC did however confirm that the correct blending ratios were used as a decreasing shift in the temperature of the HDPE melting peak was observed accompanied by an increasing LDPE melting peak with LDPE inclusion. Percentage crystallinity of a film was therefore not a good means of predicting permeability. Fractional free volume on the other hand is much more accurate in predicting

permeability in films, especially when the effects of added substance play a determining role in a macro property. These results are shown in Figure 6.2. POM was also attempted but did not yield in any significant or usable results.

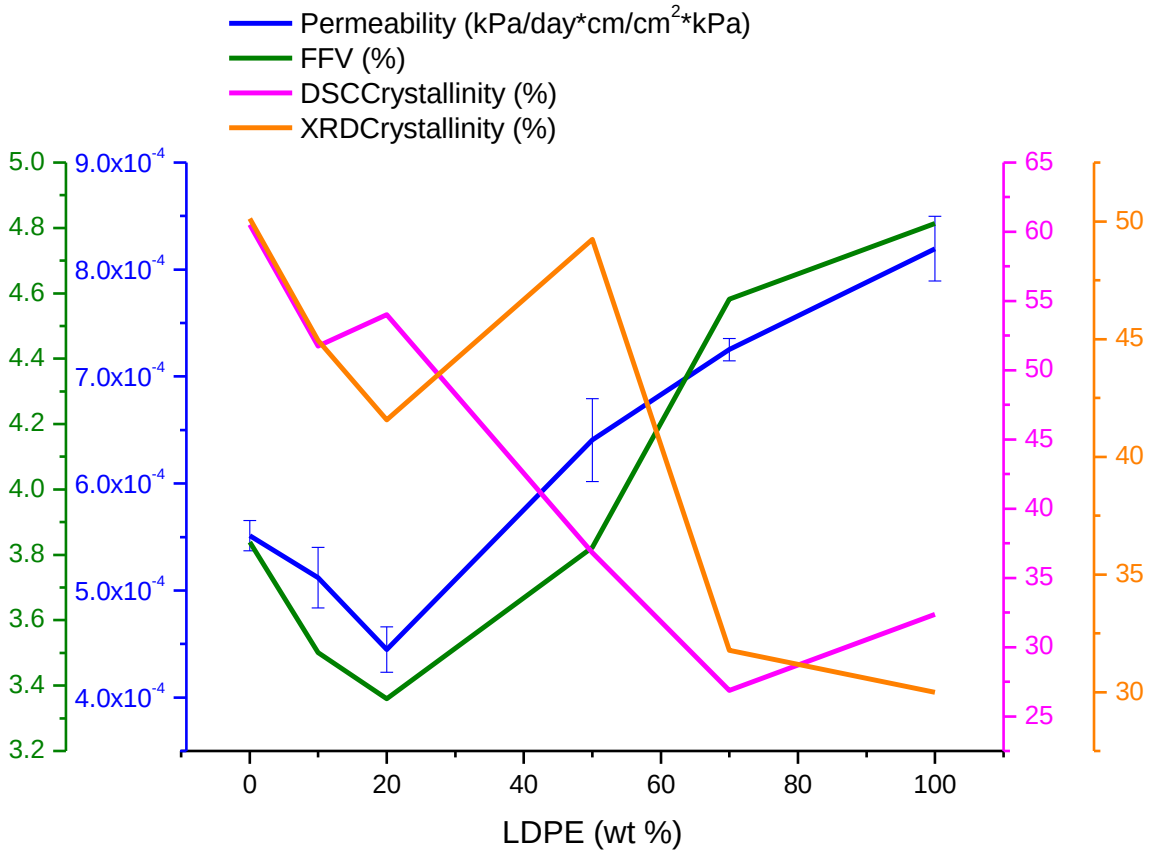

Figure 6.2: Combined graph of all the results in part three (HDPE:LDPE).

The study was successful in setting up an envelope for permeability and mechanical properties of a range of commonly used polyolefins. Within this envelope a specific range of properties was targeted. Determination of how morphology influenced the permeability two sample sets were then convincingly correlated via positron annihilation spectroscopy. Crystallinity studies from DSC and XRD experiments did not show a good relationship with permeability. From XRD experiments however the crystal form did yield in a good correlation with permeability in part two. Polarized-light worked well for imaging of PP crystals but the resolution was too low for HDPE:LDPE blends. Overall the FFV experiments showed the best results in predicting a polymers permeability.

6.2 Future work

The results obtained from this study are very promising especially the PALS studies in combination with permeability of polymeric films. ^{13}C NMR spectroscopy as done by Botha et al.[1] should also be used to probe the rigid amorphous phase of these films to highlight exactly how the FFV behaves at the interfacial boundaries. Although some work has been done in relating permeability to FFV for homopolymers on the basis of different functional groups and different gasses[2,3], investigation into blends and copolymers of low cost polyolefins have not been studied extensively. The trend in permeability seen in part three with low LDPE concentrations could be of great importance to the packaging industry. With the food packaging industry being the main consumer of plastic in the world, any advances in this field will be highly valuable. Future work can therefore be done on different blends or copolymer compositions to further increase the envelope of known materials.

Polarized-light microscopy also worked well for imaging of the HEPCs, but the resolution was too low for the HDPE:LDPE blends. Greater magnification or even scanning electron microscopy could be used for a more detailed view of the particles.

Although there was a focus shift during the middle stages of this study away from dunnage bags and more towards the fundamental impact of morphology on permeability the mechanical properties should be correlated to that of permeability for application based purposes for example the application of dunnage bags require a much higher mechanical strength than that of food packaging.

6.3 References

1. Botha, L. and Van Reenen, A. J. The effect of in-process ethylene incorporation on the evolution of particle morphology and molecular characteristics of commercial heterophasic ethylene propylene copolymers (HEPCs). *Eur. Polym. J.* **49,** 2202–2213 (2013).

2. Thran, A., Kroll, C. and Faupel, F. Correlation between fractional free volume and diffusivity of gas molecules in glassy polymers. *J. Polym. Sci. Part B Polym. Phys.* **37,** 3344–3358 (1999).

3. Park, J. Y. and Paul, D. R. Correlation and prediction of gas permeability in glassy polymer membrane materials via a modified free volume based group contribution method. *J. Memb. Sci.* **125,** 23–39 (1997).

Appendix

1.1 Tensile test results

Example of a stress-strain curve for each sample

Figure A1: LDPE

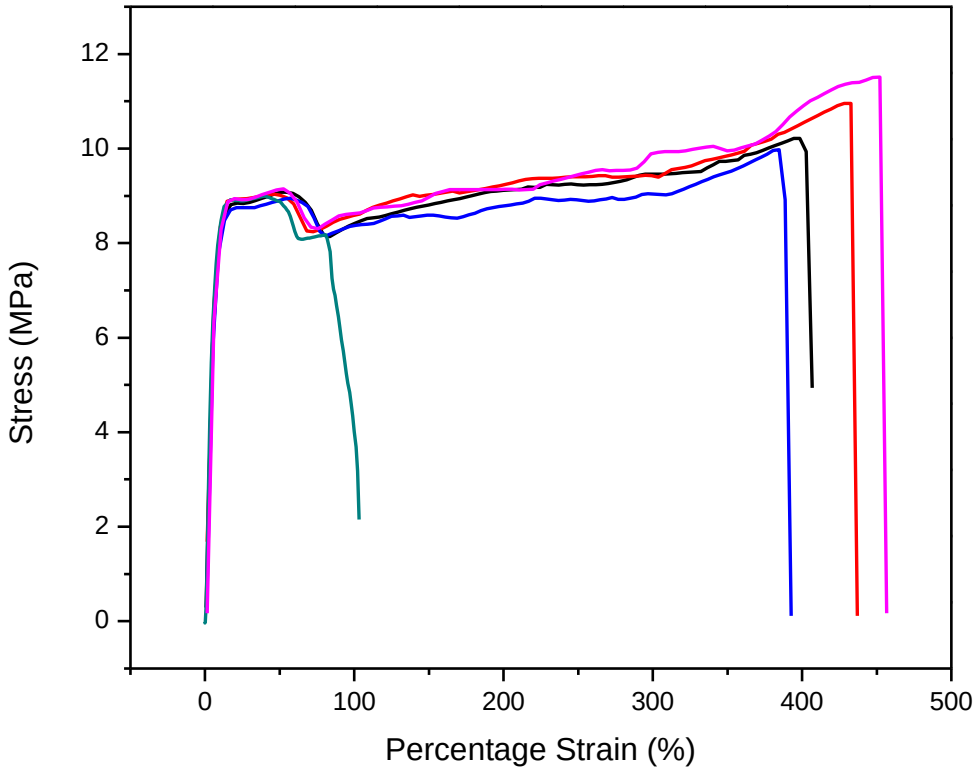

Figure A2: iPP

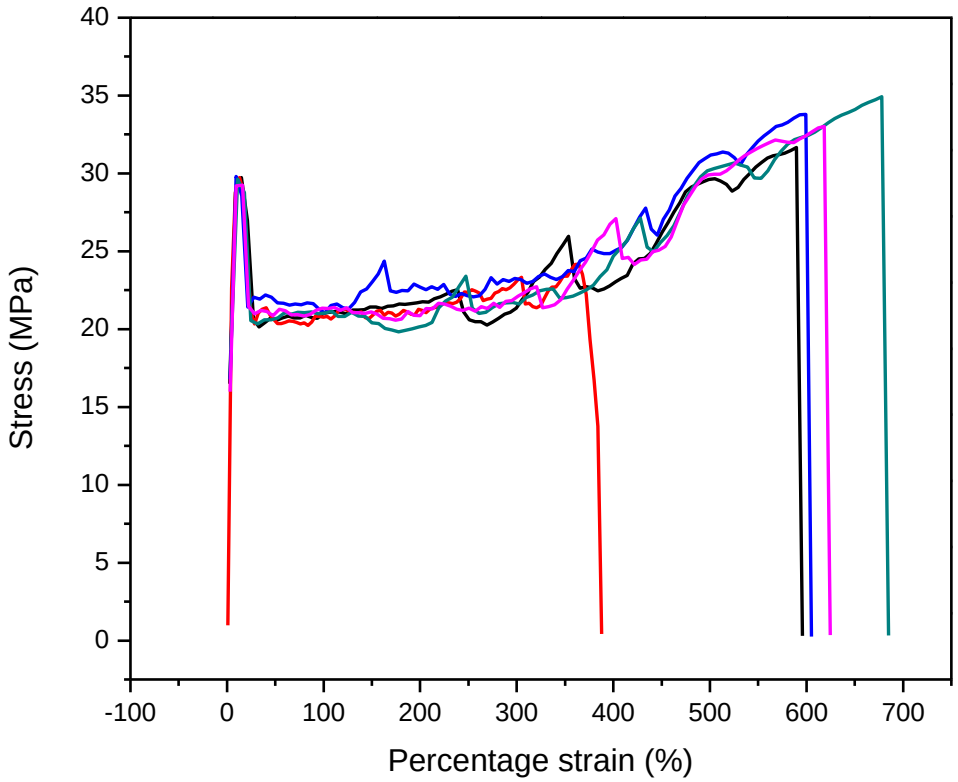

Figure A3: CMR348

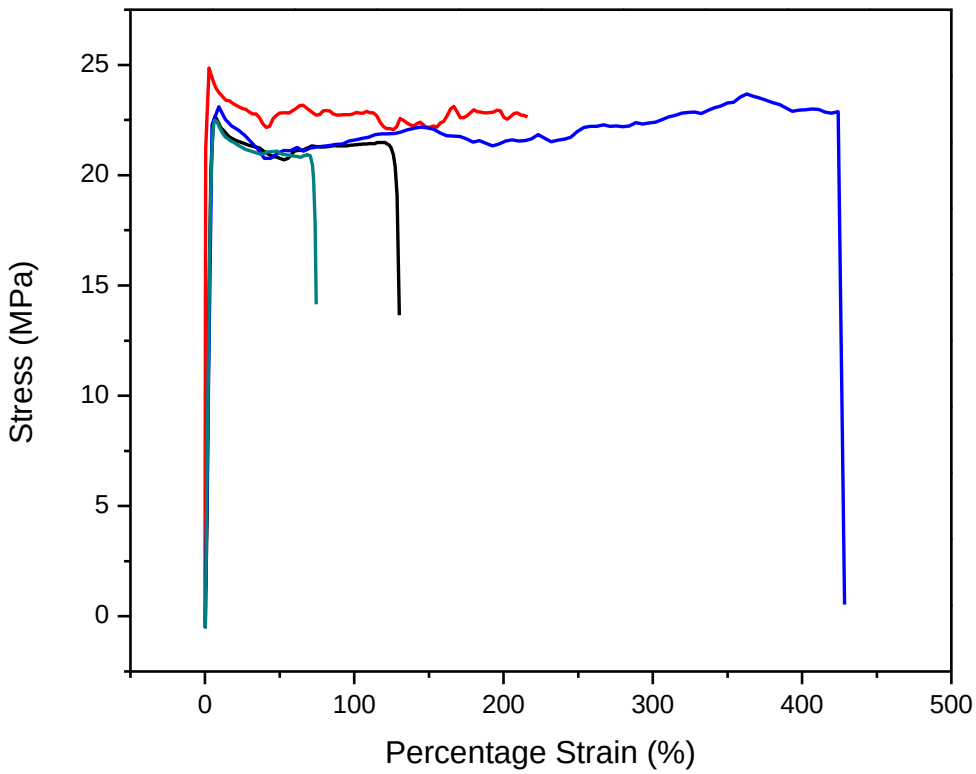

Figure A4: CMR648

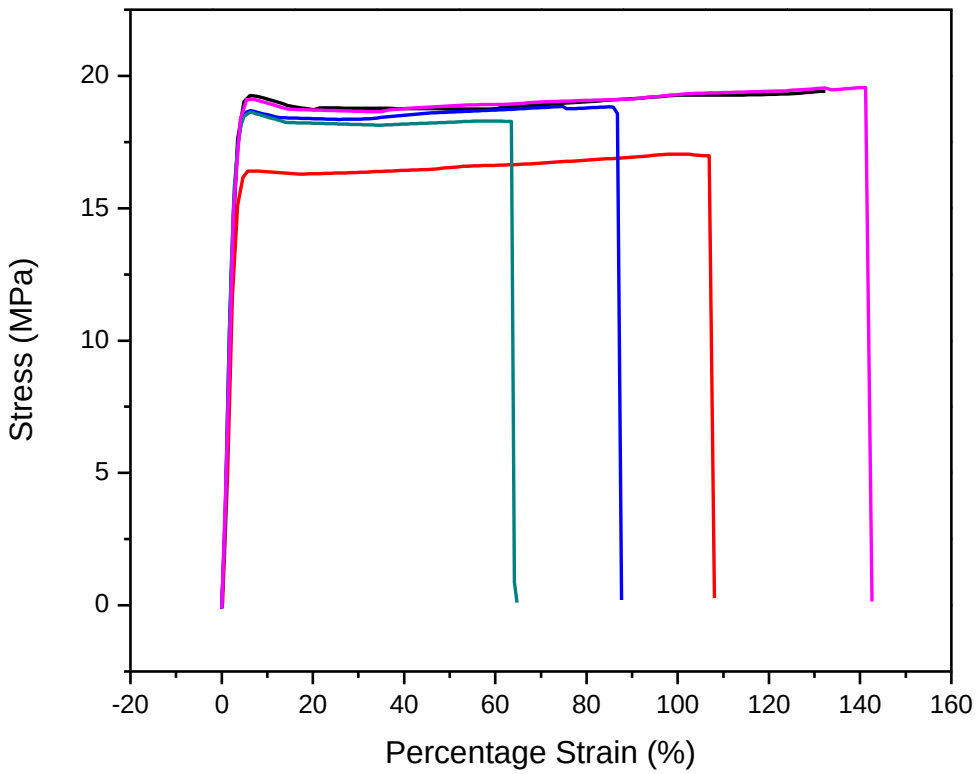

Figure A5: EVOH44

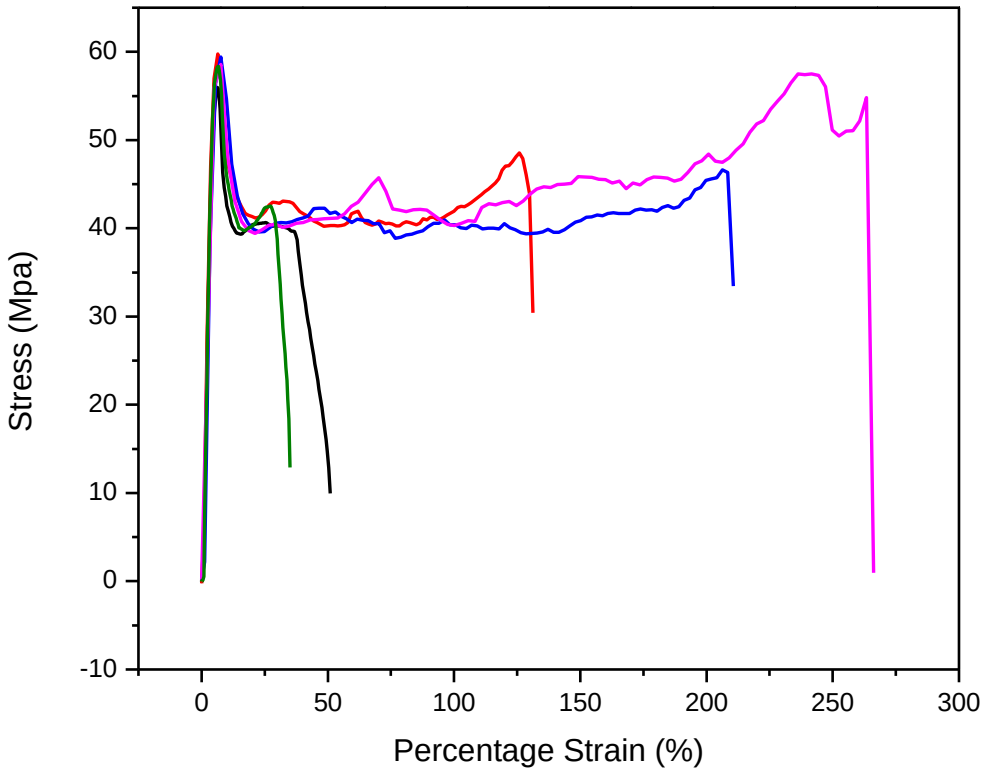

Figure A6: EVOH27

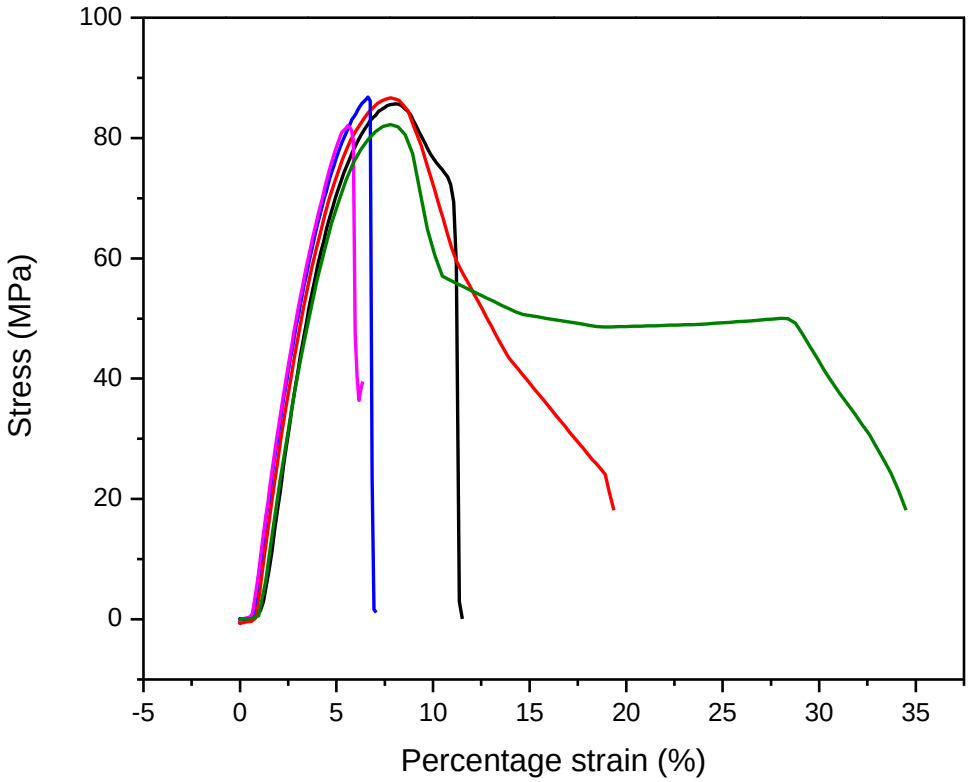

Figures A7: Permeability test method calibration

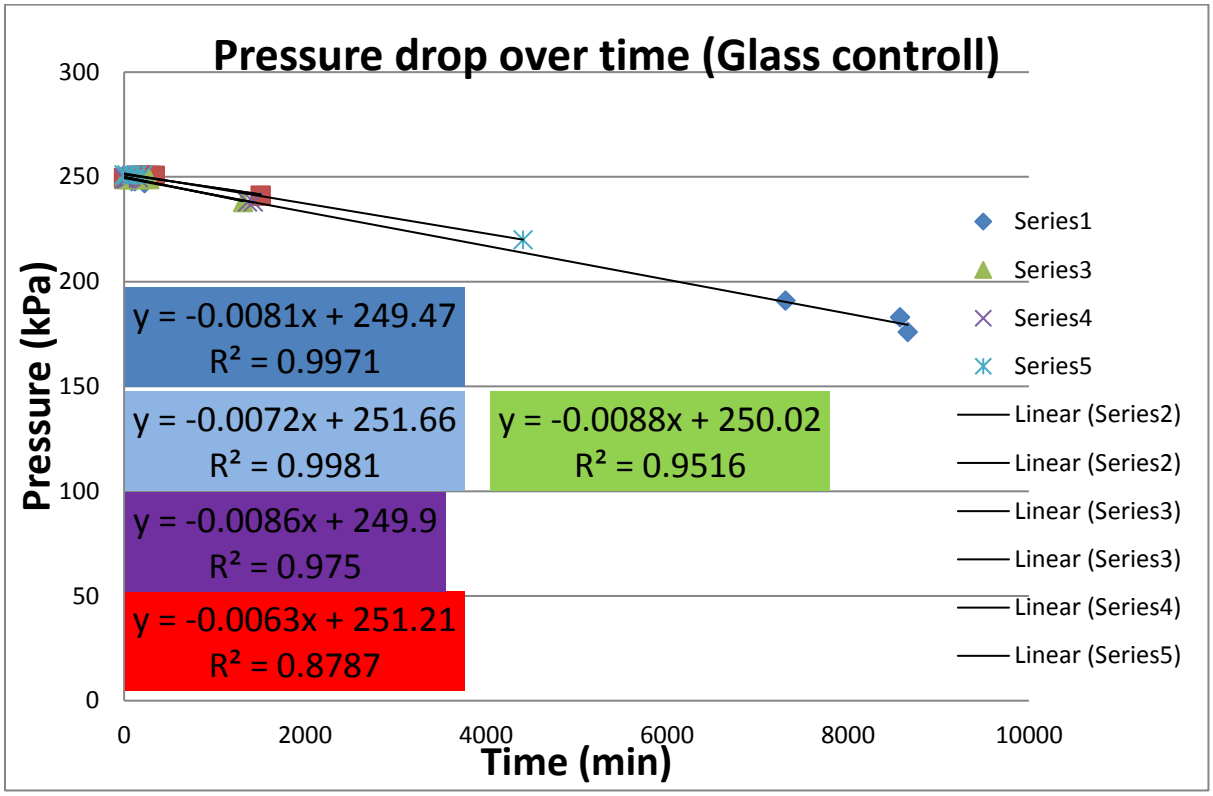

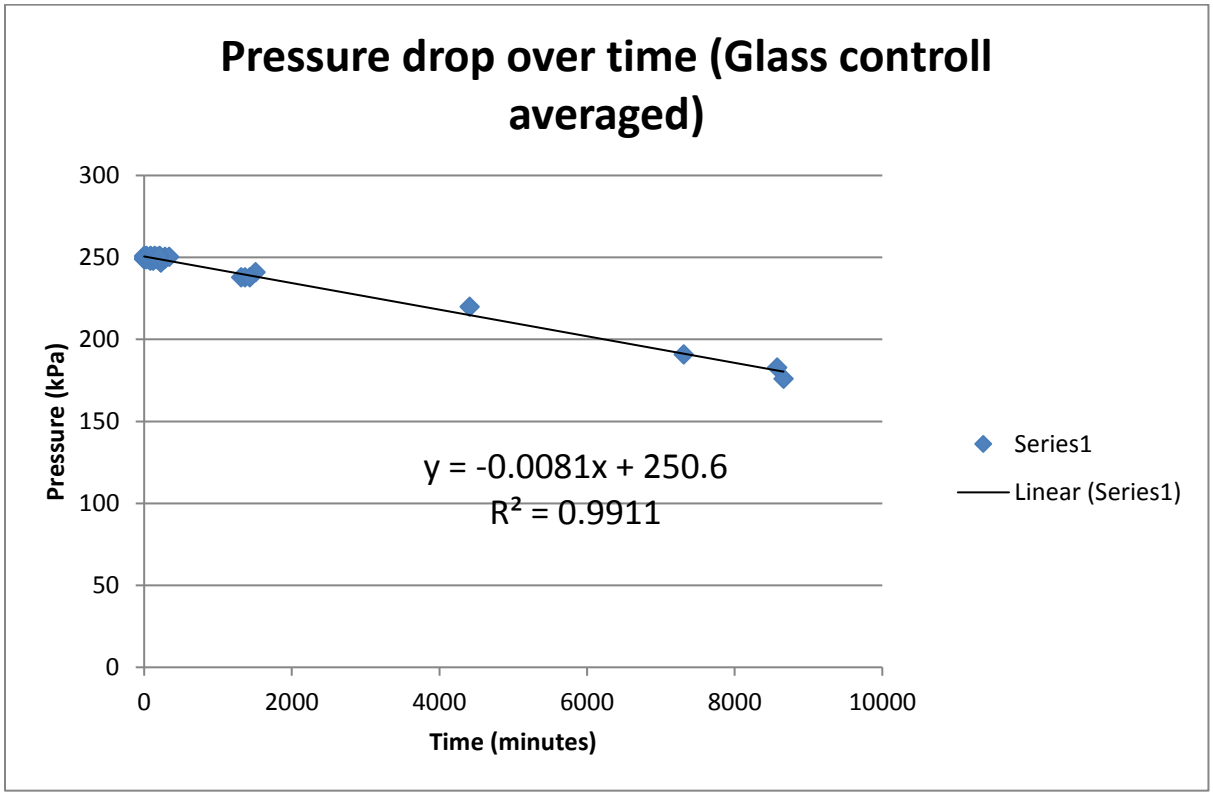

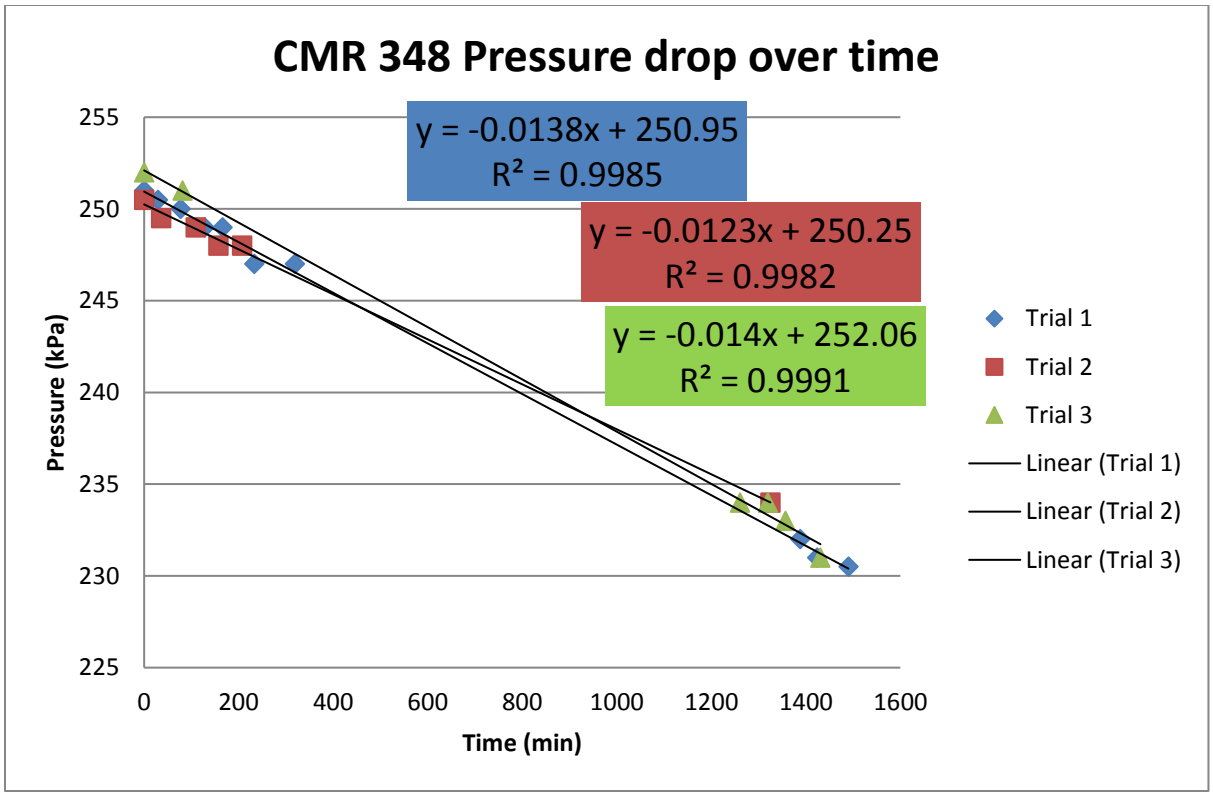

P= (measured rate-glass average rate)*thickness/ (Area*(Pressure difference))

Conventional measurement of permeability via mass transport of gas:

$$\frac{\Delta mgas}{\Delta t} = P\frac{A\Delta p}{l}$$

P	=	Permeability of barrier
Δm gas / Δt	=	transmission rate
A	=	area of barrier
L	=	thickness of barrier
Δp	=	partial pressure difference across the barrier

Adapted measurement for pressure difference readings:

$$P = \frac{(Measured\ transmission\ rate\ through\ film - glass\ average\ rate) * l}{A * \Delta p}$$

Which results in the units for permeability being:

$$\left[\frac{\frac{kPa}{day} * cm}{cm^2 * kPa}\right]$$

Figure A8: DSC Results of Part II depicting slight endothermic peak around 120°C.